Invariants of 3-manifolds, unitary representations of the mapping class group and numerical calculations

M. Karowski, R. Schrader
Institut für Theoretische Physik
Freie Universität Berlin
E. Vogt
Institut für Mathematik
Freie Universität Berlin

August 13, 1996

Abstract

Based on previous results of the two first authors, it is shown that the combinatorial construction of invariants of compact, closed 3-manifolds by Turaev and Viro as state sums in terms of quantum $6j$-symbols for $Sl_q(2,\mathbf{C})$ at roots of unity ($q = \exp \pi i/r$) leads to the unitary representation of the mapping class group found by Moore and Seiberg. Via a Heegaard decomposition this invariant may therefore be written as the absolute square of a certain matrix element of a suitable group element in this representation. For an arbitrary Dehn surgery on a figure-eight knot we provide an explicit form for this matrix element involving just one $6j$-symbol. This expression is analyzed numerically and compared with the conjectured large $k = r - 2$ asymptotics of the Chern-Simons-Witten state sum [1], whose absolute square is the Turaev-Viro state sum. In particular we find numerical agreement concerning the values of the Chern-Simons invariants for the flat SU(2) connections as predicted by the asymptotic expansion of the state sum with analytical results found by Kirk and Klassen [2].

1 Introduction

The advent of topological quantum field theories has stimulated the analysis of compact 3-manifolds and knot theory. Thus Witten ([1], see also King and Fröhlich [3]) suggested

a functional integral approach using the Chern-Simons action (with a coupling constant $k \in \mathbf{Z}$, called the level) to obtain Jones' polynomial knot invariants [4] as expectation values of Wilson loops. In particular the partition function $\tau(M,k)$ itself should give rise to new invariants of 3-manifolds M. The idea of Witten was made rigorous by Reshetikhin and Turaev [5][6] without recourse to the as yet formal functional integral approach by using the theory of braided ribbon graphs associated to quantum groups, in particular for the quantum group $SL_q(2,\mathbf{C})$ at roots of unity ($q = \exp \pi i/r, r = k+2$). The correct normalization of the Reshetikhin-Turaev invariants was provided by Kirby and Melvin [7], who also analyzed these invariants for small r.

Another approach, at first sight seemingly unrelated, has been advocated by Turaev and Viro [8] (and investigated further by Turaev [9][10]) using quantum $6j$-symbols, in particular those of $SL_q(2,\mathbf{C})$ at roots of unity. This approach was generalized in [11] and [12] to a large class of algebras (replacing $SL_q(2,\mathbf{C})$) with associated 6j-symbols. Using a triangulation of a closed 3-manifold M, they define an invariant, called a state sum in analogy to partition functions in statistical mechanics, and then show the independence of the particular triangulation, thus giving rise to an invariant $Z(M,r)$. As it turned out, for closed, *oriented* compact 3-manifolds, the case we shall be dealing with exclusively in this article, the relation

$$Z(M, r = k+2) = |Z_{C.S.}(M,k)|^2 \tag{1.1}$$

between the Turaev-Viro invariant and the Chern-Simons-Witten invariant holds [9], [13].

The construction in [8] was extended in [14] to the case where M is not necessarily closed. Furthermore in [15] a direct proof was given exhibiting the Turaev-Viro theory as a topological quantum field theory with a Hilbert space structure given in terms of a suitably formulated reflexion positivity property [16]. For an extension of these results to quantum group versions of arbitrary semisimple Lie groups and an alternative proof of eq. (1.1) see [17].

Using the representations of $SL(2,\mathbf{Z})$ (the mapping class group for the torus) as given by Gepner and Witten [18], Freed and Gompf [19] and Jeffrey [20] have analyzed the Chern-Simons-Witten invariants for lens spaces and torus bundles over S^1. In fact, each of these invariants are then just given as a certain matrix element of a suitable mapping class group element in this representation which is obtained from the appropriate Heegaard decomposition. It also involves the use of the canonical framing given by Atiyah [21].

One aim of this article is to show in Section 3 that the Turaev Viro approach for $SL_q(2,\mathbf{C})$ and arbitrary $q = \exp(i\pi/r)$ leads to a unitary representation of the mapping class group for Riemann surfaces of arbitrary genus. In fact, these representations parametrized by r are exactly those found by Moore and Seiberg [22] in the context of

conformal quantum field theory. Via a suitable Heegard decomposition the Turaev-Viro invariant $Z(M,r)$ may be written in accordance with relation (1.1) as the absolute square of a suitable matrix element of a mapping class group element in the given representation. Our discussion so far does not permit the conclusion that the matrix element itself defines an invariant. This is related to the fact that the Turaev-Viro invariant is frame independent. Our result confirms preliminary findings of Kohno [23] who started the opposite way by first defining representations of the mapping class group and then by showing that certain matrix elements define invariants.

For the readers convenience in Section 2 we briefly recapitulate the main concepts and results in [15]. In particular we will use certain bases in the topological quantum field theory associated to the Turaev-Viro approach. These bases are given in terms of invariants of so called coloured graphs on the boundary of an arbitrary oriented, compact 3-manifold. The mapping class group representations considered in Section 3 are then defined in a natural way as linear transformations on this set of invariants of graphs. In Section 4 we shall give a more detailed description for the case when M is obtained via an (n/m) Dehn surgery on a figure-eight knot. In that case $Z(M,r)$ is given as the absolute square of an expression which involves a 3-fold sum over colours and with only one 6j-symbol. The resulting expression for $Z(M,r)$ cannot be simplified further in an analytic way. In Section 5, however, and stimulated by the computer calculations on lens spaces carried out by Freed and Gompf [19], we present results from a numerical analysis for manifolds M obtained in this way and which in particular include some hyperbolic manifolds. In particular, we use our results to calculate Chern-Simons invariants of associated flat $SU(2)$-bundles over these manifolfds as predicted by the conjecture on the asymptotic behaviour as $k \to \infty$ of the Chern-Simons-Witten state sum and compare these with the analytic results of Kirk and Klassen [2]. Kirk and Klassen present tables for five Dehn surgeries on the figure-8-knot. But it is easy to extend their calculations of Chern-Simons invariants to any Dehn surgery. In all cases considered the calculations based on their method and our numerical calculation, which is based on a fundamentally different approach, give up to precision bounds identical results concerning the values of the Chern-Simons actions for flat bundles. Also we confirm the different asymptotic behaviour of the contributions to the state sum resulting from the irreducible and the reducible flat connections, respectively, as predicted by stationary phase methods applied to the formal functional integral. The coefficients of this asymptotic expansion are related to the Reidemeister torsion of the flat bundle. In principle our numerical results also permit the evaluation of these coefficients. This could be another check of the validity of this asymptotic expansion which has not been performed so far. We note that in the case of

lens spaces, Jeffrey [20] has performed an analytic calculation of the Chern-Simons action based on Gauss' reciprocity theorem and found agreement with the well known analytic results on the flat $SU(2)$-bundles.

In the present case the relevance of the Turaev-Viro invariants of hyperbolic spaces for the associated fundamental groups (contained in $SL(2,\mathbf{C})$) and the associated number theory remains an open question.

2 Invariants of coloured graphs

In this section we give a brief review of the construction of coloured graphs in the context of the Turaev-Viro approach as given in [15]. First we recall the construction of invariants of graphs on 2-manifolds as boundaries of 3-manifolds. Let $|G|$ be the topological space associated to a 1-dim. simplicial complex G (see e.g. [24]). By assumption on G every vertex $\sigma^0 \in G$ is contained in the boundary of $n = n(\sigma^0)$ 1-simplexes in G with $2 \leq n \leq 4$ and we will call σ^0 an n-vertex. The notion of being an n-vertex with $n \geq 3$ is independent of the particular triangulation G of $|G|$. Every 4-vertex σ^0 is given an additional structure by pairing the four 1-simplexes meeting in σ^0 into two unordered pairs. The two 1-simplexes in one pair are called opposite to each other. In addition one of the pairs is given the name "above" and the other pair the name "below" and is depicted in Fig. 1. By

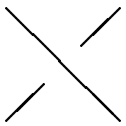

Figure 1: *The additional structure at a 4-vertex*

the above remark this additional structure is independent of the particular triangulation G of $|G|$. By abuse of notation we continue to denote by $|G|$ this space equipped with this additional structure.

Let $\underline{x} : \sigma^1 \mapsto x(\sigma^1)$ be a map from the set of non-oriented 1-simplexes in G into the set of "colours" $\mathcal{I} = \{0, \frac{1}{2}, 1, \frac{3}{2}, \ldots, \frac{r}{2} - 1\}$ with the following properties.

1) If two 1-simplexes σ_1^1 and σ_2^1 join at a 2-vertex, then $x(\sigma_1^1) = x(\sigma_2^1)$.

2) If two 1-simplexes σ_1^1 and σ_2^1 are opposite to each other at a 4-vertex then $x(\sigma_1^1) = x(\sigma_2^1)$ (compare Fig. 1).

If sdG is a subdivision of G, then such a map $\underline{x}$ induces a map $sd\underline{x}$ on sdG with similar properties by setting $sdx(\sigma^{1'}) = x(\sigma^1)$ whenever $|\sigma^{1'}| \subset |\sigma^1|$ $(\sigma^{1'} \in sdG, \sigma^1 \in G)$. We say

that $\underline{x}$ on G and $\underline{x}'$ on G' with $|G| = |G'|$ are equivalent if they induce the same map on a common subdivision. The equivalence class is called a coloured graph, denoted by $|G|_{\underline{x}}$. Any set ℓ in $|G|$ homeomorphic to an interval and not containing any n-vertex ($n \geq 3$) will be called a line. For given $|G|_{\underline{x}}$, by condition 1) to each line we may associate a colour $x = x(\ell)$. By definition a coloured graph on a 2-manifold Σ is a pair $(|G|_x, \varphi)$, where φ is a homeomorphism of $|G|$ into Σ with the following additional property. Near the image $\varphi(\sigma^0)$ of a 4-vertex σ^0, the images of the two open opposite 1-simplexes $\in G$ in one pair are separated by the images of the closed one simplex G in the other pair for any choice of a triangulation G of $|G|$ (compare Fig. 1). Two coloured graphs $(|G|_{\underline{x}}, \varphi)$ and $(|G|_{\underline{x}}, \varphi')$ on Σ are called isotopic if there is a homotopy φ_t $(0 \leq t \leq 1)$ of the maps φ and φ' such that $(|G|_{\underline{x}}, \varphi_t)$ are coloured graphs on Σ for all $0 \leq t \leq 1$.

In [15] a generalization of the state sum $Z(M, r)$ of Turaev and Viro for the case $SL_q(2, \mathbf{C})$ ($q = \exp i\pi/r$) was given in the form of assigning a complex number $Z(M, |G|_{\underline{x}}, \varphi)$ (depending on r) to each triple $(M, |G|_{\underline{x}}, \varphi)$ where $(|G|_{\underline{x}}, \varphi)$ is a coloured graph on ∂M, with M being an oriented, compact 3-manifold. Moreover $Z(M, |G|_{\underline{x}}, \varphi)$ defined as a state sum is a homotopy invariant of the pair $(|G|_{\underline{x}}, \varphi)$. This understood and identifying $|G|$ with its image in ∂M under φ, the above state sum is also simply written as $Z(M, |G|_{\underline{x}})$.

Example 2.1 *Some examples of Viro-Turaev invariants of 3-manifolds which will be used in the following are (see e.g. [14] and [15]):* $Z(D^3) = 1$, $Z(S^3) = w^{-2}$, $Z(S^2 \times S^1) = 1$, $Z(S^1 \times S^1 \times S^1) = (r-1)^2$, $Z(M \setminus D^3) = w^2 Z(M)$, *where w is defined later (see eq. (2.13)).*

Lemma 2.2 *In [14] and [15] (see also [25]) factorization formulas were derived for the invariants of 3-manifolds equipped with coloured graphs.*

a) If a 3-manifold consists of two disconnected parts $M \cap M' = \emptyset$ such that $|G|_{\underline{a}} \subset \partial M$ and $|G'|_{\underline{a}'} \subset \partial M'$, then

$$Z(M \cup M', |G|_{\underline{a}} \cup |G|'_{\underline{a}'}) = Z(M, |G|_{\underline{a}}) Z(M', |G|'_{\underline{a}'}). \tag{2.2}$$

b) If $|G|_{\underline{a}}$ is planar, i.e. if $|G|$ is contained in an open set of ∂M homeomorphic to a disc, then $Z(M, |G|_{\underline{a}})$ factorizes, i.e. the relation

$$Z(M, |G|_{\underline{a}}) = Z(M)\, Z(|G|_{\underline{a}}) \tag{2.3}$$

holds (see Theorem 4.2 in [15]). Here $Z(|G|_{\underline{a}})$ is independent of M and is called the invariant of the planar graph $|G|_{\underline{a}}$. Since for the unit ball D^3 in $\mathbf{R}^3$ with boundary

$\cong S^2$) $Z(D^3) = 1$ *(see Example 2.1), we have*

$$Z(|G|_{\underline{a}}) = Z(D^3, |G|_{\underline{a}}). \tag{2.4}$$

This expression is not only homotopy invariant but also invariant under Reidemeister moves.

c) If a graph consists of disconnected planar parts $|G_1|_{\underline{a}} \cap |G_2|_{\underline{b}} = \emptyset$

$$Z(|G_1|_{\underline{a}} \cup |G_2|_{\underline{b}}) = Z(|G_1|_{\underline{a}}) Z(|G_2|_{\underline{b}}) \ . \tag{2.5}$$

We also recall some examples of invariants of planar graphs which will be used later. The invariant of the circle with colour i

$$Z\left(\bigcirc\!\!\!

Lemma 2.3 *The invariant of any planar graph is the sum of products of invariants of the simple graphs of eqs. (2.6-2.9); i.e. it can be expressed in terms of w_i^2, q_i and the 6j-symbols.*

In [15] the construction of $Z(M, |G|_{\underline{x}})$ was also extended to coloured graphs in the interior of the 3-manifold M by the following

Definition 2.4 *Let M be a compact 3 manifold. A coloured graph $\mathcal{G}_{\underline{x}}$ in M is a triple $(c(\mathcal{G}_{\underline{x}}), \mathcal{T}_{\mathcal{G}_{\underline{x}}}, |G|_{\underline{x}})$ where*

a) $c(\mathcal{G}_{\underline{x}})$ is a finite 1-dim. simplicial complex embedded in int M and called the core of $\mathcal{G}_{\underline{x}}$.

b) $\mathcal{T}_{\mathcal{G}_{\underline{x}}}$ is an open tubular neighborhood of $c(\mathcal{G}_{\underline{x}})$ in int (M) with smooth boundary $\partial\mathcal{T}_{\mathcal{G}_{\underline{x}}}$.

c) $|G|_{\underline{x}}$ is a coloured graph on $\partial\mathcal{T}_{\mathcal{G}_{\underline{x}}}$.

Given $\mathcal{G}_{\underline{x}}$ we denote by $M \setminus \mathcal{T}_{\mathcal{G}_{\underline{x}}}$ the compact oriented 3-manifold obtained by deleting $\mathcal{T}_{\mathcal{G}_{\underline{x}}}$ from M. By construction the boundary of $M \setminus \mathcal{T}_{\mathcal{G}_{\underline{x}}}$ is the disjoint union of $\partial\mathcal{T}_{\mathcal{G}_{\underline{x}}}$ and ∂M. By definition the invariant of the 3-manifold M equipped with a coloured graph in its interior is

$$Z(M(\mathcal{G}_{\underline{x}})) = Z(M \setminus \mathcal{T}_{\mathcal{G}_{\underline{x}}}, |G|_{\underline{x}}). \tag{2.11}$$

Of course this definition may be extended to the case where there is another coloured graph $|G'|_{\underline{x}'}$ on ∂M. This notion of a coloured graph $\mathcal{G}_{\underline{x}}$ in M allows the introduction of what has been called a meridian m in [15]. By definition it is given as follows.

Definition 2.5 *Consider a subset in $\mathcal{T}_{\mathcal{G}_{\underline{x}}}$ which looks like int $D^2 \times I$ (D^2 the unit disc in $\mathbf{R}^2$, $I = [0,1]$ the unit interval) such that its intersection with $\partial\mathcal{T}_{\mathcal{G}_{\underline{x}}}$ has the form $(S^1 = \partial D^2) \times I$. Then a meridian m is any circle of the form $S^1 \times \{Q\}$ $(Q \in (0,1) \subset I)$. Such a meridian will be equipped with a colour y and combined with $|G|_{\underline{x}}$ to give a coloured graph denoted by $|G \cup m|_{\underline{x},y}$. Given several such meridians written as $\underline{m} = m_1 \cup \ldots \cup m_n$ and equipped with colours $\underline{y} = (y_1, \ldots, y_n)$ by definition the invariant of the 3-manifold M containing the graph $\mathcal{G}^{\underline{m}}_{\underline{x}} = (c(\mathcal{G}_{\underline{x}}), \mathcal{T}_{\mathcal{G}_{\underline{x}}}, |G \cup \underline{m}|_{\underline{x},\underline{y}})$ with meridians $\underline{m}$ is*

$$Z(M(\mathcal{G}^{\underline{m}}_{\underline{x}})) = \sum_{\underline{y}} \prod_{i=1}^{n} \frac{w_{y_i}^2}{w^2} Z(M \setminus \mathcal{T}_{\mathcal{G}_{\underline{x}}}, |G \cup \underline{m}|_{\underline{x},\underline{y}}), \tag{2.12}$$

where

$$w^2 = \sum_i w_i^4 = \frac{-2r}{(q - q^{-1})^2}\ , \quad q = e^{i\pi/r}. \tag{2.13}$$

and w_i^2 is given by eq. (2.6). A line of $\mathcal{G}^m_{\underline{x}}$ is called oriented if it intersects a meridian once transversally. It is called left (right) handed if it undercrosses (overcrosses) the meridian in the sense of Fig. 1, looking from the exterior of $\mathcal{T}_{\mathcal{G}_{\underline{x}}}$ onto the 4-vertex.

Graphically a left-handed and a right-handed line look locally like

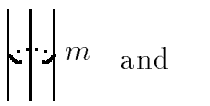

We recall also of following properties of meridians (Corollaries 5.5, 5.6 and 6.5 of ref. [15]) which will be used later.

Lemma 2.6 *The following projecting and branching properties of meridians hold:*

i) If one of the colours x in $\underline{x}$ happens to be simultaneously left and right handed, the invariant (2.12) vanishes unless $x = 0$.

$$\sum_{yy'} \frac{w_y^2}{w^2}\frac{w_{y'}^2}{w^2}$$

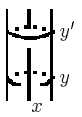

$$\propto \delta_{x0}$$

ii) If m and m' are two meridians of the same say left handed line, one of them may be omitted

$$m \cup m' \equiv m \quad \text{or}$$

$$. \tag{2.14}$$

iii) If three say left handed lines with meridians m, m' and m'' branch at a three vertex, one of the meridians may be omitted

$$m \cup m' \cup m'' \equiv m \cup m' \quad \text{or}$$

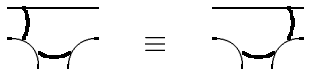

$$. \tag{2.15}$$

Analogous relations hold for right handed lines. The relations above have to be understood in the sense, that both sides will give the same invariant in formula (2.12). In the following all lines will be assumed to be oriented. We write for short $Z(M, \mathcal{G}_{\underline{a},\underline{\bar{b}}})$ if the graph has left handed lines with colours $\underline{a}$ and right handed ones with colours $\underline{\bar{b}}$. Also we have the following

Lemma 2.7 *[15] The relative braiding of a left- and a right-handed line is trivial:*

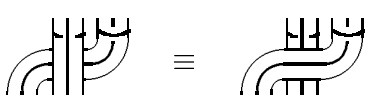

$$.$$

Corollary 2.8 *A graph $\mathcal{G}_{\underline{a},\underline{b}}$ in S^3 with oriented lines can be decomposed as $\mathcal{G}_{\underline{a}} \cup \mathcal{G}_{\underline{b}}$ such that $\mathcal{G}_{\underline{a}} \subset D_1^3$, $\mathcal{G}_{\underline{b}} \subset D_2^3$ and $D_1^3 \cap D_2^3 = \emptyset$. Therefore the invariant factorizes*

$$Z\Big(S^3(\mathcal{G}_{\underline{a},\underline{b}})\Big) = w^2\, Z\Big(S^3(\mathcal{G}_{\underline{a}})\Big)\, Z\Big(S^3(\mathcal{G}_{\underline{b}})\Big)\ . \tag{2.16}$$

In addition in [15] formulas were derived which express the change of the invariants of 3-manifolds (equipped with graphs) under specific changes $M \to M'$ of the manifolds.

Lemma 2.9 Cutting "full cylinders": *If the 3-manifold M contains a cylinder $D^2 \times [0,1]$ such that $\partial D^2 \times [0,1] \subset \partial M$ and (for a point $P \in \partial D^2$) $P \times [0,1]$ is part of a line (of colour a) of a graph $G_{\underline{a}}$, then the cylinder may be removed using the formula*

$$Z\left(\begin{array}{c}\includegraphics[height=2.2cm]{fig_cut_full_cylinder_lhs.pdf}\\ \begin{array}{l}M\\ b\\ a\\ c\\ M\end{array}\end{array}\right) = \delta_{a0}\,\frac{1}{w_b w_c}\, Z\left(\begin{array}{c}\includegraphics[height=2.2cm]{fig_cut_full_cylinder_rhs.pdf}\\ \begin{array}{l}M'\\ b\\ c\\ M'\end{array}\end{array}\right)$$

Lemma 2.10 Introducing "hollow tubes": *If the 3-manifold M contains a cylinder $D^2 \times [0,1]$ such that $D^2 \times \{0,1\} \subset \partial M$, then the cylinder may be removed (i.e. a tube may be introduced) using the formula*

$$Z\left(\begin{array}{c}\includegraphics[height=2.2cm]{fig_hollow_tubes_lhs.pdf}\\ M\end{array}\right) = \sum_x w_x^2\, Z\left(\begin{array}{c}\includegraphics[height=2.2cm]{fig_hollow_tubes_rhs.pdf}\\ \begin{array}{l}M'\\ x\\ M'\end{array}\end{array}\right)$$

where the circle $\partial D^2 \times \{1/2\}$ with colour x is a meridian.

Finally we have a relation between invariants of graphs in the internal of 3-manifolds and the invariants of planar graphs. For the simple case of S^3 this is given by the following theorem.

Theorem 2.11 *For any graph $\mathcal{G}_{\underline{a}} \subset S^3$ (of only left-handed lines) the invariant of $S^3(\mathcal{G}_{\underline{a}})$ may be written in terms of the invariant of a corresponding planar graph $|G|_{\underline{a}}$ on S^2*

$$Z\Big(S^3(\mathcal{G}_{\underline{a}})\Big) = w^{\chi(\mathcal{G}_{\underline{a}})-2}\, Z(|G|_{\underline{a}}) \tag{2.17}$$

where $\chi(\mathcal{G}_{\underline{a}})$ is the Euler characteristics of the graph $\mathcal{G}_{\underline{a}}$ and $|G|_{\underline{a}}$ is some projection of $\mathcal{G}_{\underline{a}} \subset S^3$ onto an $S^2 \subset S^3$.

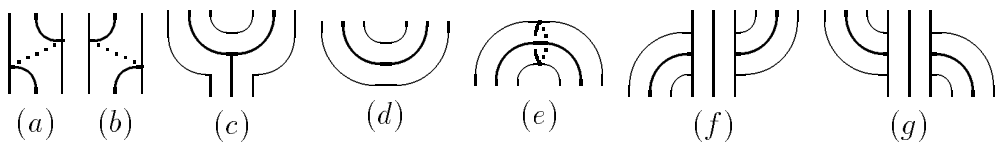

Figure 2: *The building stones of any graph* $\mathcal{G}_{\underline{a}}$.

The exact form of the planar graph $|G|_{\underline{a}}$ follows from the construction in the proof.

Proof: We use homotopy invariance, iteratively the Wigner-Eckart relation (2.10) and change the graph $\mathcal{G}_{\underline{a}} \subset S^3$ such that its projection onto $\mathbf{R^2}$ may be decomposed into local pieces which look like those of Fig. 2. Note that all meridians may be shifted by Lemma 2.6 such that they only appear at pieces of type (e). Now we use the properties of the meridians (see [15] Lemma 5.4) to change the pieces of Fig. 2 $(a), (b)$ as

Creating a hole in S^3 such that its projection lies completely below the the projection of the graph, the invariant changes by a factor w^{-2}: $Z\Big(S^3(\mathcal{G}_{\underline{a}})\Big) = w^{-2}\, Z\Big((S^3 \setminus D^3)(\mathcal{G}_{\underline{a}})\Big)$ (see Example 2.1). Now we deform the hole such that finally the original position of the graph lies completely inside the hole. During this procedure we perform step by step several changes of the graph and the manifold. At the end the tubular neighborhood has disappeared and only the hole remains with the graph $|G|_{\underline{a}}$ on its boundary S^2. If, during this procedure, we reach a piece of type (d) we apply Lemma 2.10 to connect it with the hole.

Where for the second step again Lemma 2.6 has been used. Thus the invariant has changed by a factor of w^2. Passing pieces of type $(a), (b), (f)$ and (g) the invariant will not change. In case of (f) we use again Lemma 5.4 of [15] to obtain

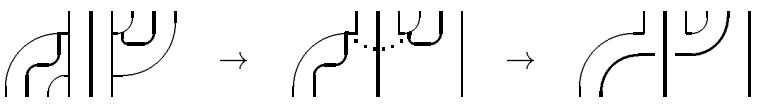

and analogously for case (g). If we reach a piece of type (e) we apply Lemma 2.9

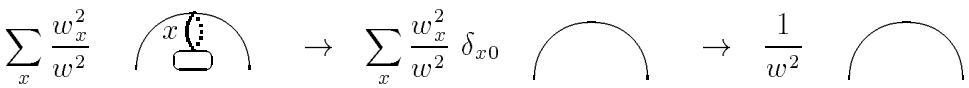

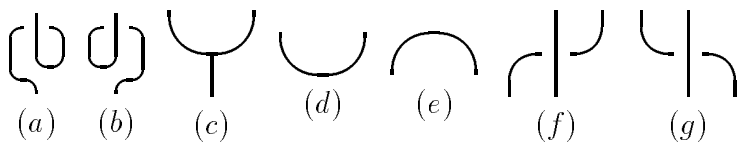

Figure 3: *The building stones of the planar graph* $|G|_{\underline{a}}$ *which correspond to* $\mathcal{G}_{\underline{a}} \subset S^3$.

The invariant changes by a factor w^{-2}. Finally the graph $\mathcal{G}_{\underline{a}}$ has disappeared and instead we have the new planar graph $|G|_{\underline{a}}$ on the boundary $\cong S^2$ where each piece of $\mathcal{G}_{\underline{a}}$ as depicted in Fig. 2 is replaced by the corresponding piece of $|G|_{\underline{a}}$ as depicted in Fig. 3. Since $Z(S^3 \setminus D^3) = 1$ and twice the number of pieces of type (e) minus twice the number of pieces of type (d) is the Euler characteristics of $\mathcal{G}_{\underline{a}}$ the claim follows.

For a graph $\mathcal{G}_{\underline{\bar{b}}} \subset S^3$ with only right-handed lines the result is quite similar. The only difference is that for the resulting planar graph $|G|_{\underline{\bar{b}}} \subset S^2$ in case of $(a), (b), (f)$ and (g) overcrossing and undercrossing is exchanged. This means that the invariant has the complex conjugate value compared to the corresponding left-handed case.

We now define basic graphs in the interior of handle bodies. We use here a slight modification of Definition 7.5 in [15]. This modification turns out to be more convenient for our construction of the representation of the mapping class group.

Consider the handle body (gefillte pretzel) M_{Σ^g} associated to a Riemann surface Σ^g of genus $g \geq 2$. Let $(\alpha_1, \ldots, \alpha_g, \beta_1, \ldots, \beta_g)$ be a canonical homology basis of Σ^g realized as simple closed curves on Σ^g such that $\alpha_1, \ldots, \alpha_g$ are contractible in M_{Σ^g}. We depict this in Fig. 4, where an additional curve α_{g+1} has been added.

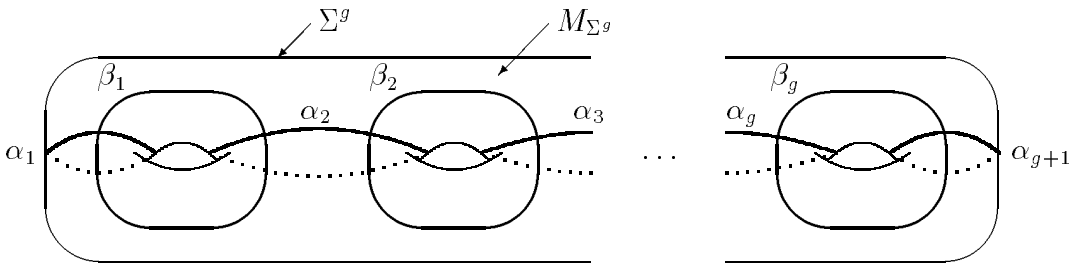

Figure 4: *A canonical homology basis* $(\alpha_1, \ldots, \alpha_g, \beta_1, \ldots, \beta_g)$ *plus the additional curve* α_{g+1}

Definition 2.12 *For the handle body* M_{Σ^g} *the canonical coloured graph* $\mathcal{G}^{\Sigma^g}_{\underline{e}} = (c(\mathcal{G}_{\underline{e}}), \mathcal{T}_{\mathcal{G}_{\underline{e}}}, |G \cup T_{\underline{\alpha}}|_{\underline{e},\underline{x}})$ *is defined as follows. It's core is of the form as depicted in Fig. 5. The coloured graph* $|G^{\Sigma^g}|_{\underline{e}}$ *with colours* $\underline{e} = (e_1, \ldots, e_{3g-3})$ *for* $(g > 1)$ *on the boundary of the tubular neighbourhood of the core is depicted in Fig. 6. In addition there are the meridians* $T_{\alpha_1}, \ldots, T_{\alpha_{3g-3}}$ *such that all lines of* $\mathcal{G}^{\Sigma^g}_{\underline{e}}$ *are left handed.*

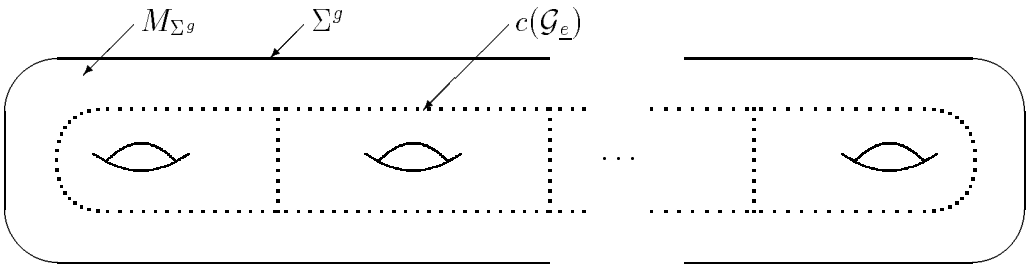

Figure 5: *The core* $c(\mathcal{G}_{\underline{e}}^{\Sigma^g})$ *= dotted line*

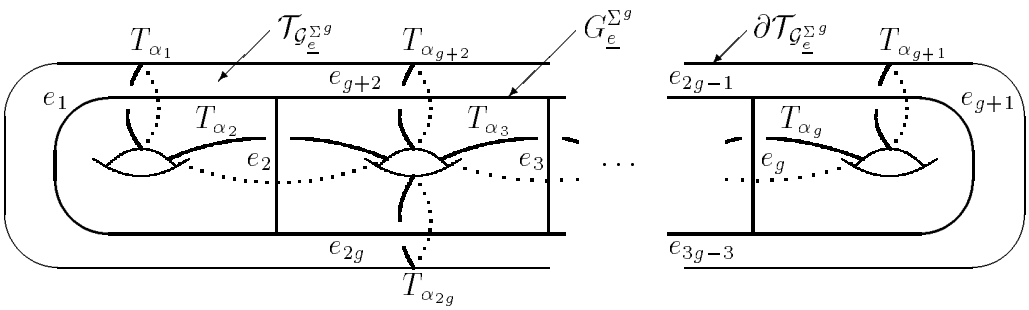

Figure 6: *The graph* $|G^{\Sigma^g}|_{\underline{e}}$ *and the meridians* $T_{\alpha_1},\ldots,T_{\alpha_{3g-3}}$

The tubular neighbourhood $\mathcal{T}_{\mathcal{G}_{\underline{e}}^{\Sigma^g}}$ of the core is a deformation retract of M_{Σ^g} and lies in a tubular neighborhood of $\Sigma^g = \partial M_{\Sigma^g}$ in M_{Σ^g}. On $\partial\mathcal{T}_{\mathcal{G}_{\underline{e}}^{\Sigma^g}}$ which is diffeomorphic to Σ^{g*} (where * means the opposite orientation). The family of curves $\alpha_1,\ldots,\alpha_{3g-3}$ extending the family $\alpha_1,\ldots,\alpha_{g+1}$ form a maximal set of disjoint (noncontractible in $\partial\mathcal{T}_{\mathcal{G}_{\underline{e}}^{\Sigma^g}}$ but contractible in $\mathcal{T}_{\mathcal{G}_{\underline{e}}^{\Sigma^g}}$) pairwise nonisotopic, nonintersecting smooth circles on $\partial\mathcal{T}_{\mathcal{G}_{\underline{e}}^{\Sigma^g}}$. Thus they define a marking whose dual graph (see e.g. [23]) is given by Fig. 5. Note that $|G^{\Sigma^g}|_{\underline{e}}$ is not uniquely fixed by the dual graph (whose homeomorphic image it is), but we shall agree that a given choice has been made such that the line corresponding to the colour e_i intersects the curve α_i exactly once ($1 \le i \le 3g-3$) and no other α_j ($j \ne i$). Now all lines with colours $e_1,\ldots,e_{3g-3}$ are assumed to be left handed with respect to the meridians $T_{\alpha_1},\ldots,T_{\alpha_{3g-3}}$ defined by the curves $\alpha_1,\ldots,\alpha_{3g-3}$.

Let $\bar{\mathcal{G}}_{\underline{\bar{f}}}^{\Sigma^g}$ be another canonical graph in M_{Σ^g} of the same form. However, now all the colours $\underline{\bar{f}} = (\bar{f}_1,\ldots\bar{f}_{3g-3})$ are right handed w.r.t. the corresponding meridians. The tubular neighbourhoods $\mathcal{T}_{\mathcal{G}_{\underline{e}}^{\Sigma^g}}$ and $\mathcal{T}_{\bar{\mathcal{G}}_{\underline{\bar{f}}}^{\Sigma^g}}$ may be taken to be disjoint. Alternatively, they may be identified, written as $\mathcal{T}_{\mathcal{G}^{\Sigma^g}}$, and the invariant (2.12) will change by a factor w^{-2g+2} only. In the following we will assume the second choice. For short we write the invariant of any 3-manifold equipped with the canonical graph as

$$Z(M(\mathcal{G}_{\underline{e},\underline{\bar{f}}}^{\Sigma^g})) \quad \text{where} \quad \mathcal{G}_{\underline{e},\underline{\bar{f}}}^{\Sigma^g} = \mathcal{G}_{\underline{e}}^{\Sigma^g} \cup \bar{\mathcal{G}}_{\underline{\bar{f}}}^{\Sigma^g}. \tag{2.18}$$

In particular we have for all colours equal to zero

$$Z(M(\mathcal{G}^{\Sigma^g}_{\underline{0},\underline{0}})) = w^{2-2g}\, Z(M). \tag{2.19}$$

Here the rule has been used how to fill "empty" tubes by Lemma 2.9 and eqs. (2.12) and (2.15) (see also Appendix A).

Finally the colours $\underline{e}$ and $\underline{\bar{f}}$ are only restricted by the fusion rules, i.e.

$$N^{e_1}_{e_2 e_{g+2}} = N^{e_3}_{e_{g+2} e_{g+3}} \ldots = N^{\bar{f}_1}_{\bar{f}_2 \bar{f}_{g+2}} = N^{\bar{f}_3}_{\bar{f}_{g+2} \bar{f}_{g+3}} \ldots = 1 \tag{2.20}$$

is supposed to hold. Here N^i_{jk} is the fusion matrix of eq. (2.7).

We introduce the handle body $M^*_{\Sigma^g}$ with the opposite orientation, equipped with the mirror graph $\mathcal{G}^{\Sigma^{g^*}}_{\underline{e}',\underline{\bar{f}}'}$ such that gluing $M^*_{\Sigma^g}$ and M_{Σ^g} along Σ^g we have

$$(M^*_{\Sigma^g} \setminus \mathcal{T}_{\mathcal{G}^{\Sigma^{g^*}}}) \underset{\Sigma^g}{\cup} (M_{\Sigma^g} \setminus \mathcal{T}_{\bar{\mathcal{G}}^{\Sigma^g}}) \cong \Sigma^g \times I \qquad (I = [0,1]) \tag{2.21}$$

and

$$\begin{aligned} |G^{\Sigma^{g^*}}|_{\underline{e}',\underline{\bar{f}}',\underline{x}'} &:= |G^{\Sigma^{g^*}} \cup \bar{G}^{\Sigma^{g^*}} \cup T^*_{\underline{\alpha}'}|_{\underline{e}',\underline{\bar{f}}',\underline{x}'} \subset \Sigma^g \times \{0\}, \\ |G^{\Sigma^g}|_{\underline{e},\underline{\bar{f}},\underline{x}} &:= |G^{\Sigma^g} \cup \bar{G}^{\Sigma^g} \cup T_{\underline{\alpha}}|_{\underline{e},\underline{\bar{f}},\underline{x}} \subset \Sigma^g \times \{1\}, \end{aligned} \tag{2.22}$$

where both graphs are homotopic in $\Sigma^g \times [0,1]$. In Appendix A we prove the orthogonality relation

$$\begin{aligned} Z\left((M^*_{\Sigma^g} \underset{\Sigma^g}{\cup} M_{\Sigma^g})(\mathcal{G}^{\Sigma^{g^*}}_{\underline{e}',\underline{\bar{f}}'} \cup \mathcal{G}^{\Sigma^g}_{\underline{e},\underline{\bar{f}}})\right) &= \sum_{\underline{x}',\underline{x}} \prod_{i=1}^{3g-3} \frac{w^2_{x'_i}}{w^2} \frac{w^2_{x_i}}{w^2} Z(\Sigma^g \times I, |G^{\Sigma^{g^*}}|_{\underline{e}',\underline{\bar{f}}',\underline{x}'} \cup |G^{\Sigma^g}|_{\underline{e},\underline{\bar{f}},\underline{x}}) \\ &= w^{-2g+2} \delta_{\underline{e}',\underline{e}} \delta_{\underline{\bar{f}}',\underline{\bar{f}}} \prod_{i=1}^{3g-3} w^{-2}_{e_i} w^{-2}_{\bar{f}_i}, \end{aligned} \tag{2.23}$$

with $\delta_{\underline{e}',\underline{e}} = \prod_{i=1}^{3g-3} \delta_{e'_i,e_i}$ (for $g > 1$) and analogously for $\delta_{\underline{\bar{f}}',\underline{\bar{f}}}$. Here and in similar situations below, we make the convention that $\mathcal{G}^{\Sigma^g}_{\underline{e},\underline{\bar{f}}}$ lies in M_{Σ^g} and $\mathcal{G}^{\Sigma^{g^*}}_{\underline{e}',\underline{\bar{f}}'}$ lies in $M^*_{\Sigma^g}$.

In the context of a topological quantum field theory any oriented compact 3-manifold M_2 with $\partial M_2 = \Sigma^g$ gives rise to a vector $|\, M_2 \,\rangle$ in a finite dimensional vector space V^{Σ^g}. Its dual $(V^{\Sigma^g})^*$ is canonically isomorphic to $V^{\Sigma^{g^*}}$ with elements $\langle\, M_1 \,|$ $(\partial M^*_1 \cong \Sigma^{g^*})$ such that the canonical pairing in $V^{\Sigma^{g^*}} \times V^{\Sigma^g}$ is given as

$$\langle\, M_1 \,|\, M_2 \,\rangle = Z(M^*_1 \underset{\Sigma^g}{\cup} M_2).$$

Furthermore if we consider a handle body equipped with its canonical graph we have the maps

$$\begin{aligned} \mathcal{G}^{\Sigma^g}_{\underline{e},\underline{\bar{f}}} &\mapsto |\,\underline{e},\underline{\bar{f}}\,\rangle = w^{g-1}\,|\,M_{\Sigma^g}(\mathcal{G}^{\Sigma^g}_{\underline{e},\underline{\bar{f}}})\,\rangle \in V^{\Sigma^g}, \\ \mathcal{G}^{\Sigma^{g^*}}_{\underline{e},\underline{\bar{f}}} &\mapsto \langle\,\underline{e},\underline{\bar{f}}\,| = w^{g-1}\langle\, M_{\Sigma^g}(\mathcal{G}^{\Sigma^g}_{\underline{e},\underline{\bar{f}}})\,| \in V^{\Sigma^{g^*}} \end{aligned} \tag{2.24}$$

such that

$$\begin{aligned} \langle\, M_1\,|\,\underline{e},\underline{\bar{f}}\,\rangle &= w^{g-1}\prod_{i=1}^{3g-3} w_{e_i}\, w_{\bar{f}_i}\, Z\left((M_1^* \underset{\Sigma^g}{\cup} M_{\Sigma^g})(\mathcal{G}^{\Sigma^g}_{\underline{e},\underline{\bar{f}}})\right), \\ \langle\,\underline{e},\underline{\bar{f}}\,|\,M_2\,\rangle &= w^{g-1}\prod_{i=1}^{3g-3} w_{e_i}\, w_{\bar{f}_i}\, Z\left((M^*_{\Sigma^g} \underset{\Sigma^g}{\cup} M_2)(\mathcal{G}^{\Sigma^{g^*}}_{\underline{e},\underline{\bar{f}}})\right) \end{aligned} \tag{2.25}$$

and by eq. (2.23)

$$\langle\,\underline{e}',\underline{\bar{f}'}\,|\,\underline{e},\underline{\bar{f}}\,\rangle = \delta_{\underline{e}',\underline{e}}\,\delta_{\underline{\bar{f}'},\underline{\bar{f}}}\,. \tag{2.26}$$

In particular we have by eq. (2.19)

$$|\,M_\Sigma\,\rangle = w^{g-1}\,|\,\underline{0},\underline{0}\,\rangle = w^{2g-2}\,|\,M_{\Sigma^g}(\mathcal{G}^{\Sigma^g}_{\underline{0},\underline{0}})\,\rangle. \tag{2.27}$$

One of the main results in [15] was the completeness relation in terms the following surgery formula

$$\langle\, M_1\,|\,M_2\,\rangle = \sum_{\underline{e}\,\underline{\bar{f}}} \langle\, M_1\,|\,\underline{e},\underline{\bar{f}}\,\rangle\langle\,\underline{e},\underline{\bar{f}}\,|\,M_2\,\rangle. \tag{2.28}$$

In other words, the vectors $|\,\underline{e},\underline{\bar{f}}\,\rangle$ and $\langle\,\underline{e},\underline{\bar{f}}\,|$ form a system of dual bases in V^{Σ^g} and $V^{\Sigma^{g^*}}$, respectively.

Remark 2.13 *This completeness relation also extends to the case when M_1 and (or) M_2 contains coloured graphs (with meridians) and (or) if M_1 and M_2 contain additional boundary components along which no gluing takes place.*

Lemma E of [15] combined with (2.23) and the fact that $w_i^* = (-1)^{2i}w_i$ shows that the antilinear extension of the map $|\,\underline{e},\underline{\bar{f}}\,\rangle \mapsto \langle\,\underline{e},\underline{\bar{f}}\,|$ (for $g > 1$) gives a map τ_{Σ^g} from V^{Σ^g} onto $V^{\Sigma^{g^*}}$ with $\tau_{\Sigma^g}\,|\,M_2\,\rangle = \langle\,M_2\,|$ and such that the resulting hermitean form (note that $\langle\,M_1\,|\,M_2\,\rangle^* = \langle\,M_2\,|\,M_1\,\rangle$) is positive definite.

Finally by the results in [15] for the dimensions of these spaces we have the relation

$$\dim V^{\Sigma^g} = \left(\mathrm{trace}\Big(\sum_{a\in\mathcal{I}}(N^a)^2\Big)^{g-1}\right)^2, \tag{2.29}$$

where the N^a are the fusion matrices given by eq. (2.7). The square on the r.h.s. of eq. (2.29) also suggests to introduce the following structure. Let $V_l^{\Sigma^g}$ and $V_r^{\Sigma^g}$ be the subspaces of V^{Σ^g} spanned by elements of the form

$$\begin{aligned} |\,\underline{e}\,\rangle &:= |\,\underline{e},\underline{0}\,\rangle, \\ |\,\underline{\bar{f}}\,\rangle &:= |\,\underline{0},\underline{\bar{f}}\,\rangle, \end{aligned} \tag{2.30}$$

respectively, such that

$$\dim V_l^{\Sigma^g} = \dim V_r^{\Sigma^g} = \text{trace}\,(\vec{N}^2)^{g-1}. \tag{2.31}$$

Then there is a canonical linear isomorphism between $V_l^{\Sigma^g} \otimes_{\mathbf{C}} V_r^{\Sigma^g}$ and V^{Σ^g} by which $|\,\underline{e}\,\rangle \otimes |\,\underline{\bar{f}}\,\rangle$ corresponds to $|\,\underline{e},\underline{\bar{f}}\,\rangle$. Also $V_{l(r)}^{\Sigma^{g^*}} = (V_{l(r)}^{\Sigma^g})^*$. The Hilbert space structure induced by τ_{Σ^g} is obviously compatible with this isomorphism. In the following section we show that the representation of the mapping class group defined on V^{Σ^g} also is compatible with this isomorphism, i.e. it factorizes with respect to the left and right handed spaces.

3 Finite dimensional unitary representations of the mapping class group

The aim of this section is to show that the results in [15] on the Turaev-Viro theory, as recalled in Section 2, lead to a unitary representation on V^{Σ^g} of the mapping class group MCG^g for Σ^g. It suffices to consider the case $g \geq 2$ since for $g = 1$ the construction is well known ([18], see also Appendix A in [15]). Let φ be a diffeomorphism of Σ^g. We define the linear transformation $\pi(\varphi)$ on V^{Σ^g} by its matrix elements

$$\langle\,\underline{e}',\underline{\bar{f}'}\,|\,\pi(\varphi)\,|\,\underline{e},\underline{\bar{f}}\,\rangle = w^{2g-2} \prod_{i=1}^{3g-3} w_{e_i'}\, w_{e_i}\, w_{\bar{f}_i'}\, w_{\bar{f}_i}\, Z\left((M_{\Sigma^g}^* \underset{(\Sigma^g,\varphi)}{\cup} M_{\Sigma^g})(\mathcal{G}_{\underline{e}',\underline{\bar{f}'}}^{\Sigma^{g^*}} \cup \mathcal{G}_{\underline{e},\underline{\bar{f}}}^{\Sigma^g})\right). \tag{3.32}$$

Here the symbol (Σ^g,φ) means that we glue $M_{\Sigma^g}^*$ to M_{Σ^g} by identifying $x \in \Sigma^{g^*}$ of $M_{\Sigma^g}^*$ with $\varphi^{-1}(x) \in \Sigma^g$ of M_{Σ^g}. Similar to eq. (2.23) the invariant in eq. (3.32), equals

$$\sum_{\underline{x}',\underline{x}} \prod_{i=1}^{3g-3} \frac{w_{x_i'}^2}{w^2}\,\frac{w_{x_i}^2}{w^2}\, Z((\Sigma^g \times I) \underset{(\Sigma^g,\varphi)}{\cup} (\Sigma^g \times I), |G^{\Sigma^{g^*}}|_{\underline{e}',\underline{\bar{f}}',\underline{x}'} \cup |G^{\Sigma^g}|_{\underline{e},\underline{\bar{f}},\underline{x}}) \tag{3.33}$$

In particular by eq. (2.23) $\pi(id)$ is the identity transformation on V^{Σ^g}.

Proposition 3.1 *The map $\varphi \mapsto \pi(\varphi)$ defines a representation of the diffeomorphism group of Σ^g. Its kernel contains the identity component, hence π descends to a representation of the mapping class group MCG^g also denoted by π.*

Proof: By the basic construction of state sums with coloured graphs in [15] it is easy to see that one may "move" φ to the right, i.e. the partition function in (3.33), equals

$$Z\left(\Sigma^g \times I, |G^{\Sigma^{g^*}}|_{\underline{e}',\underline{\bar{f}}',\underline{x}'} \cup \varphi(|G^{\Sigma^g}|_{\underline{e},\underline{\bar{f}},\underline{x}})\right) \tag{3.34}$$

with the following notation: $\varphi(|G^{\Sigma^g}|_{\underline{e},\underline{f},\underline{x}})$ is the 1-dim. simplicial complex in $\Sigma^g \times \{1\}$ which is the image of $|G^{\Sigma^g}|_{\underline{e},\underline{f},\underline{x}}$ under φ and equipped with the corresponding colours. Inserting (3.39) into (3.33) and (3.32) now proves the second part of the proposition for π due to the homotopy invariance for coloured graphs of state sums. The first part of the proposition follows from the observation that

$$(\Sigma^g \times I) \underset{(\Sigma^g, \varphi_1 \circ \varphi_2)}{\cup} (\Sigma^g \times I) \cong (\Sigma^g \cup I) \underset{(\Sigma^g, \varphi_1)}{\cup} (\Sigma^g \times I) \underset{(\Sigma^g, \varphi_2)}{\cup} (\Sigma^g \times I)$$

for two diffeomorphisms φ_1 and φ_2 and from the completeness relation (2.28). This concludes the proof of Proposition 3.1.

Let $A_1, \ldots, A_{3g-3}$ and $B_1, \ldots, B_g$ be the elementary Dehn twists defined by the curves $\alpha_1, \ldots, \alpha_{3g-3}$ and $\beta_1, \ldots, \beta_g$ respectively (see Figs. 4 and 6). It is known (see e.g. [26]) that MCG^g is generated by e.g. the elements $A_1, \ldots, A_g, A_{g+2}$ and $B_1, \ldots, B_g$. Furthermore let $S_i = A_{2g-2+i}^{-1} B_i A_{2g-2+i}^{-1}$ $(1 < i < g)$, $S_1 = A_1^{-1} B_1 A_1^{-1}$, $S_g = A_{g+1}^{-1} B_g A_{g+1}^{-1}$. Then MCG^g is in particular generated by the elements $A_1, \ldots, A_{3g-3}$ and $S_1, \ldots, S_g$.

Proposition 3.2 *The representation $\pi(\varphi)$ of MCG^g defined by eq. (3.32) fulfills*

$$\langle \underline{e}', \underline{\bar{f}'} \,|\, \pi(\varphi) \,|\, \underline{e}, \underline{\bar{f}} \rangle = \langle \underline{e}' \,|\, \pi_l(\varphi) \,|\, \underline{e} \rangle \langle \underline{\bar{f}'} \,|\, \pi_r(\varphi) \,|\, \underline{\bar{f}} \rangle. \tag{3.35}$$

This means π decomposes into two maps π_l and π_r on $V_l^{\Sigma^g}$ and $V_r^{\Sigma^g}$, respectively, which are defined by eq. (2.30). By use of the canonical isomorphism $V^{\Sigma^g} \cong V_l^{\Sigma^g} \otimes_{\mathbf{C}} V_r^{\Sigma^g}$, eq. (3.35) implies that

$$\pi(\varphi) \cong \pi_l(\varphi) \otimes \pi_r(\varphi). \tag{3.36}$$

Furthermore the map π_r is complex conjugate to the map π_l in these bases. For the generating elements $A_1, \ldots, A_{3g-3}, S_1, \ldots, S_g$ of MCG^g the map π_l is given by

$$\begin{aligned} \langle \underline{e}' \,|\, \pi_l(A_i) \,|\, \underline{e} \rangle &= \langle \underline{e}', \underline{0} \,|\, \pi(A_i) \,|\, \underline{e}, \underline{0} \rangle \\ \langle \underline{e}' \,|\, \pi_l(S_i) \,|\, \underline{e} \rangle &= \frac{1}{w} \langle \underline{e}', \underline{0} \,|\, \pi(S_i) \,|\, \underline{e}, \underline{0} \rangle, \end{aligned} \tag{3.37}$$

where $w = \sqrt{r/2}/(\sin \pi/r)$ (see eq. (2.13)).

Proof: By explicit calculation of the matrix elements (3.32) we prove the factorization property (3.35) for the generators of MCG^g. Thus it suffices to define π_l on these elements. We start with the elements $A_1, \ldots, A_{3g-3}$ and determine first $\pi(A_1) \,|\, \underline{e}, \underline{0} \,\rangle$. For the elementary Dehn twist A_1 along α_1, the graph $|G^{\Sigma^g}|_{\underline{e},\underline{0},\underline{x}}$ on $\partial \mathcal{T}_{G^{\Sigma^g}}$ of Fig. 6 is changed into $A_1 |G^{\Sigma^g}|_{\underline{e},\underline{0},\underline{x}}$ as given in Fig. 7. We see that the meridians $T_{\alpha_1}, \ldots, T_{\alpha_{3g-3}}$ are left unchanged. Also the equivalence of the two pictures in Fig. 7 on the level of state sums

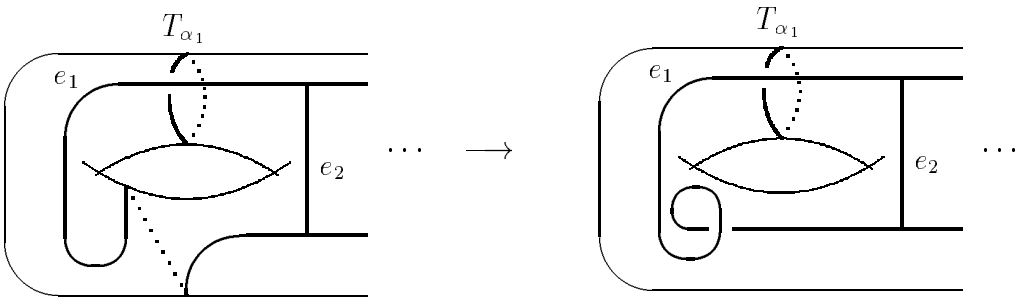

Figure 7: *The Dehn twist A_1 applied to $|G^{\Sigma^g}|_{\underline{e},\underline{0},\underline{x}}$.*

results from Lemma 5.4 in [15] (compare also the proof of Theorem 2.11). Hence we obtain by eqs. (2.9) and (2.10)

$$\pi(A_1)\,|\,\underline{e},\underline{0}\,\rangle = |\,\underline{e},\underline{0}\,\rangle\, q_{e_1}^2, \tag{3.38}$$

where $q_j = (-1)^{-j} q^{j(j+1)}$ $(j \in \mathcal{I})$. For right handed lines we would obtain a similar picture as that of Fig. 7, however, the self over crossing is replaced by the opposite version. Therefore we obtain

$$\pi(A_1)\,|\,\underline{e},\underline{\bar{f}}\,\rangle = |\,\underline{e},\underline{\bar{f}}\,\rangle\, q_{e_1}^2 q_{\bar{f}_1}^{-2}. \tag{3.39}$$

The discussion for any A_i $(1 \leq i \leq 3g-3)$ is analogous giving

$$\pi(A_i)\,|\,\underline{e},\underline{\bar{f}}\,\rangle = |\,\underline{e},\underline{\bar{f}}\,\rangle\, q_{e_i}^2 q_{\bar{f}_i}^{-2}, \quad 1 \leq i \leq 3g-3. \tag{3.40}$$

We turn to the investigation of $S_1 = A_1^{-1} B_1 A_1^{-1}$ and discuss first $\pi(S_1)\,|\,\underline{e},\underline{0}\,\rangle$. The

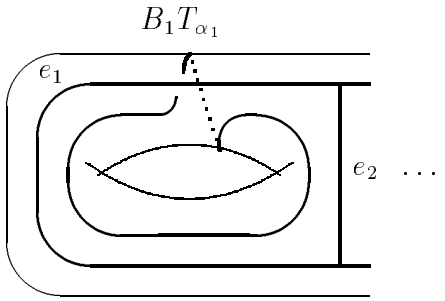

Figure 8: *The effect of B_1 on $|G^{\Sigma^g}|_{\underline{e},\underline{0},\underline{x}}$.*

graph $|G^{\Sigma^g}|_{\underline{e}}$ and the meridians $T_{\alpha_2}, \ldots, T_{\alpha_{3g-3}}$ do not change under B_1. The circle $B_1 T_{\alpha_1}$ takes the form depicted in Fig. 8. This results in the following action of S_1 on $|G^{\Sigma^g}|_{\underline{e}}$ and its meridians as depicted in Fig. 9. In particular the circle $A_1^{-1} B_1 A_1^{-1} T_{\alpha_1}$ is just

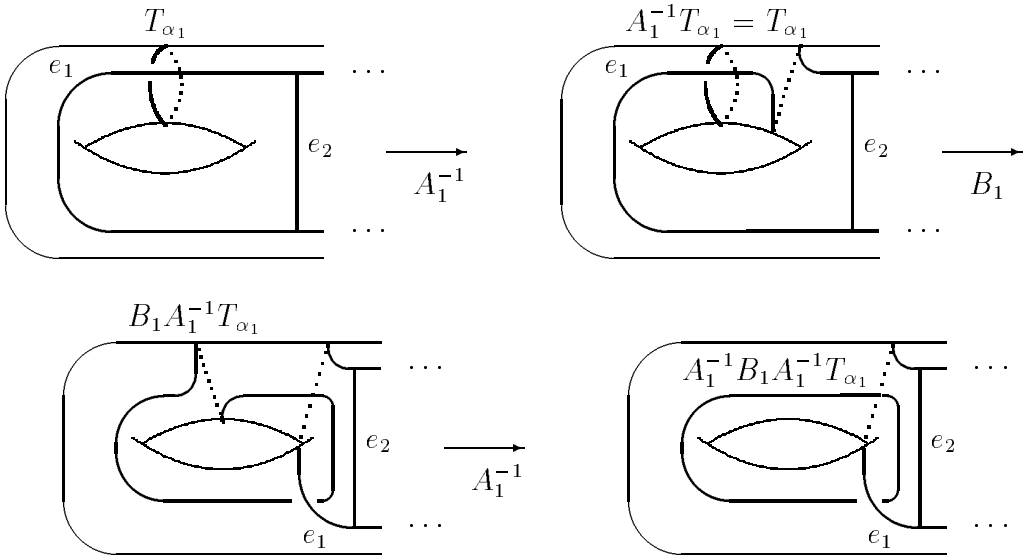

Figure 9: *The effect of* $S_1 = A_1^{-1}B_1A_1^{-1}$ *on* $|G^{\Sigma g}|_{\underline{e},\underline{0},\underline{x}}$.

β_1. To evaluate the matrix elements $\langle\, \underline{e}', \underline{\bar{f}'} \,|\, \pi(S_1) \,|\, \underline{e}, \underline{\bar{f}} \,\rangle$ we apply a, basis transformation $|\, \underline{e}, \underline{0} \,\rangle \;\mapsto\; |\, \underline{\tilde{e}}, \underline{0} \,\rangle$. First we omit the meridian T_{α_2} of e_2 by eq. (2.15). Then we use the identity (see rel. (4.11) in [15], a special case of a Fierz transformation) for the coloured graph

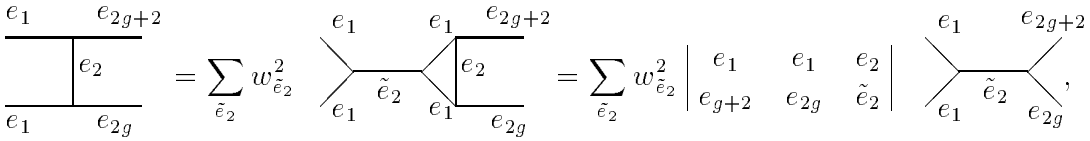

$$, \qquad (3.41)$$

where $\left| \begin{matrix} a & b & c \\ d & e & f \end{matrix} \right|$ is the 6j-symbol of eq. (2.8). We obtain the transformation matrix

$$\langle\, \underline{\tilde{e}}, \underline{0} \,|\, \underline{e}, \underline{0} \,\rangle = \prod_{i \neq 2} \delta_{\tilde{e}_i e_i} \; w_{\tilde{e}_2} w_{e_2} \left| \begin{matrix} e_1 & e_1 & e_2 \\ e_{g+2} & e_{2g} & \tilde{e}_2 \end{matrix} \right| . \qquad (3.42)$$

Also we apply the analogous transformation $\langle\, \underline{e}', \underline{0} \,| \;\mapsto\; \langle\, \underline{\tilde{e}}', \underline{0} \,|$.

Using the cutting rules established in [15] (see also Appendix A) to eqs. (3.32) and (3.33) for $\varphi = S_1$ we obtain the resulting expression

$$\langle\, \underline{\tilde{e}}', \underline{0} \,|\, \pi(S_1) \,|\, \underline{\tilde{e}}, \underline{0} \,\rangle = w^{2g-2} \prod_{i=1}^{3g-3} w_{\tilde{e}_i'} w_{\tilde{e}_i} \sum_{\underline{x}', \underline{x}} \prod_{i=1}^{3g-3} \frac{w_{x_i'}^2}{w^2} \frac{w_{x_i}^2}{w^2} Z(M_1, |G_1|) \; w^2 \frac{\delta_{\tilde{e}_2' \tilde{e}_2}}{w_{\tilde{e}_2}^2} \; Z(M_2, |G_2|), \qquad (3.43)$$

where $Z(M_1, |G_1|)$ is the invariant of the manifold and the coloured graph as depicted in Fig. 10 and $Z(M_2, |G_2|)$ that of the remainder. Here x_1 is the colour of $S_1 T_{\alpha_1}$ belonging

to the line of colour $\tilde{e}_1$ on the inner part of the surface and x_1' is the colour of the meridian for $\tilde{e}_1'$ on the outer part of the surface.

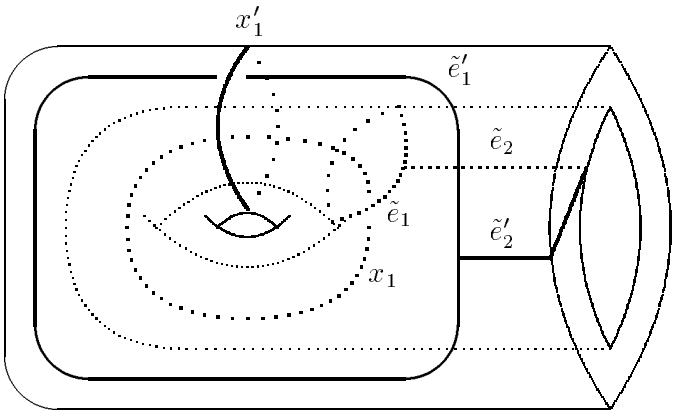

Figure 10: *Graphical description for the nontrivial contribution to the matrix element* $\langle\, \tilde{\underline{e}}', \underline{0} \,|\, \pi(S_1) \,|\, \tilde{\underline{e}}, \underline{0} \,\rangle$.

By appropriate cuttings (in analogy to the proof of (2.23) in Appendix A) we write $Z(M_1, |G_1|)$ and $Z(M_2, |G_2|)$ in terms of invariants of planar graphs and find

$$\langle\, \tilde{\underline{e}}', \underline{0} \,|\, \pi(S_1) \,|\, \tilde{\underline{e}}, \underline{0} \,\rangle = \frac{1}{w} S^{\tilde{e}_2}_{\tilde{e}_1' \tilde{e}_1} \prod_{i=2}^{3g-3} \delta_{\tilde{e}_i' \tilde{e}_i} \tag{3.44}$$

where

$$S^{\tilde{e}_2}_{\tilde{e}_1', \tilde{e}_1} = \frac{w_{\tilde{e}_1'} w_{\tilde{e}_1}}{w} Z \left(\right.$$

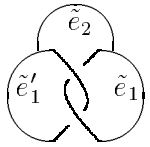

$$\left. \right) \tag{3.45}$$

in the sense of a state sum of a planar graph on S^2 (see Example 4.10 in [15]). For right lines the matrix S in eq. (3.44) is to be replaced by the conjugate complex matrix.

$$\bar{S}^{\tilde{\bar{f}}_2}_{\tilde{\bar{f}}_1', \tilde{\bar{f}}_1} = (S^{\tilde{\bar{f}}_2}_{\tilde{\bar{f}}_1', \tilde{\bar{f}}_1})^* = \frac{w_{\tilde{\bar{f}}_1'} w_{\tilde{\bar{f}}_1}}{w} Z \left(\right.$$

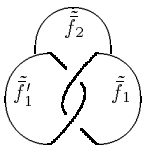

$$\left. \right) \tag{3.46}$$

By the same method as above one can calculate the general matrix element

$$\langle\, \tilde{\underline{e}}', \tilde{\underline{\bar{f}}}' \,|\, \pi(S_1) \,|\, \tilde{\underline{e}}, \tilde{\underline{\bar{f}}} \,\rangle = S^{\tilde{e}_2}_{\tilde{e}_1' \tilde{e}_1} \bar{S}^{\tilde{\bar{f}}_2}_{\tilde{\bar{f}}_1', \tilde{\bar{f}}_1} \prod_{i=2}^{3g-3} \delta_{\tilde{e}_i' \tilde{e}_i} \delta_{\tilde{\bar{f}}_i' \tilde{\bar{f}}_i} . \tag{3.47}$$

In terms of the original basis we obtain by the transformation formula (3.42)

$$\langle\, \underline{e}', \underline{\bar{f}}' \,|\, \pi(S_1) \,|\, \underline{e}, \underline{\bar{f}} \,\rangle = S^{e_{g+2}, e_{2g}}_{e_1' e_2', e_1 e_2} \bar{S}^{\bar{f}_{g+2}, \bar{f}_{2g}}_{\bar{f}_1' \bar{f}_2', \bar{f}_1 \bar{f}_2} \prod_{j=3}^{3g-3} \delta_{e_j' e_j} \delta_{\bar{f}_i' \bar{f}_i} \ , \tag{3.48}$$

where

$$
\begin{aligned}
S^{e_{g+2},e_{2g}}_{e'_1e'_2,e_1e_2} &= w_{e'_2}w_{e_2}\sum_{\tilde{e}_2} w^2_{\tilde{e}_2}
\left|\begin{matrix} e'_1 & e'_1 & e'_2 \\ e_{g+2} & e_{2g} & \tilde{e}_2 \end{matrix}\right|\left|\begin{matrix} e_1 & e_1 & e_2 \\ e_{g+2} & e_{2g} & \tilde{e}_2 \end{matrix}\right| S^{\tilde{e}_2}_{e'_1e_1} \\
&= \frac{w_{e'_1}w_{e'_2}w_{e_1}w_{e_2}}{w}\sum_{\tilde{e}_2} w^2_{\tilde{e}_2} Z\left(\right. \\
&= \frac{w_{e'_1}w_{e'_2}w_{e_1}w_{e_2}}{w} Z\left(\right) .
\end{aligned}
\tag{3.49}
$$

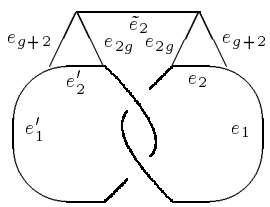

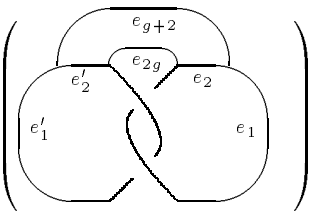

and $\bar{S} = S^*$. Here we have again made use of a Fierz transformation in the proof of the last relation in eq. (3.49).

Obviously $\pi(S_g = A^{-1}_{g+1}B_gA^{-1}_{g+1})$ may be calculated in the same way giving (compare Fig. 6)

$$
\langle \underline{e}', \underline{\bar{f}}' \,|\, \pi(S_g) \,|\, \underline{e}, \underline{\bar{f}} \rangle = S^{e_{3g-3},e_{2g-1}}_{e'_{g+1}e'_g,e_{g+1}e_g} \bar{S}^{\bar{f}_{3g-3},\bar{f}_{2g-1}}_{\bar{f}'_{g+1}\bar{f}'_g,\bar{f}_{g+1}\bar{f}_g} \prod_{\substack{i=1 \\ i\neq g,g+1}} \delta_{e'_je_j}\delta_{\bar{f}'_i\bar{f}_i} \ . \tag{3.50}
$$

It remains to calculate the matrix elements of $\pi(S_i = A^{-1}_{2g-2+i}B_iA^{-1}_{2g-2+i})$ $(1 < i < g)$. We look at the local picture around the i-th hole (see Fig. 11). The colours e_I, e_{II}, e_{III} and

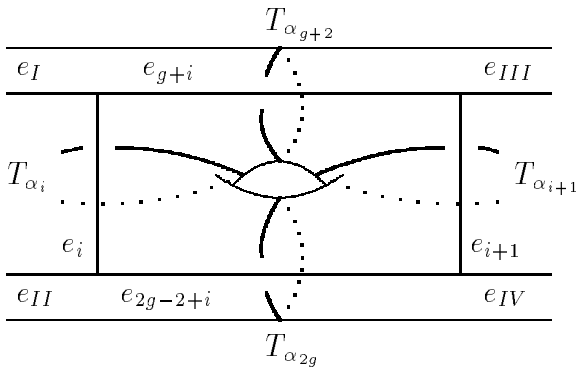

Figure 11: *The local form of* $|G^{\Sigma^g}|_{\underline{e}}$ *and its meridians around the i-th hole.*

e_{IV} in Fig. 11 are given as

$$
\begin{aligned}
e_I &= e_{g+i-1} \quad \text{if } i > 2 \\
e_{II} &= e_{2g-3+i} \quad \text{if } i > 2
\end{aligned}
$$

$$
\begin{aligned}
e_I &= e_{II} = e_1 \quad \text{if } i = 2 \\
e_{III} &= e_{g+i+1} \quad \text{if } i < g-1 \\
e_{IV} &= e_{2g-i+1} \quad \text{if } i < g-1 \\
e_{III} &= e_{IV} = e_{g+1} \quad \text{if } i = g-1
\end{aligned}
$$

By methods similar to these used to calculate the matrix elements of S_1 we obtain

$$
\langle\, \underline{e}', \underline{\bar{f}'} \,|\, \pi(S_i) \,|\, \underline{e}, \underline{\bar{f}} \,\rangle = \frac{1}{w^2} \prod_{j \in I_1} w_{e'_j} w_{e_j} w_{\bar{f}'_j} w_{\bar{f}_j} \prod_{j \in I_2} \delta_{e'_j e_j} \delta_{\bar{f}'_j \bar{f}_j} \; Z_i \cdot \bar{Z}_i, \quad (1 < i < g), \tag{3.51}
$$

where

$Z_i = Z$ 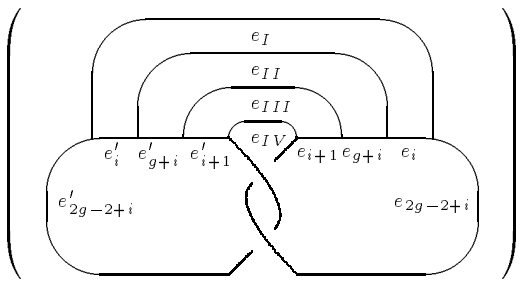

,

$\bar{Z}_i = Z_i^*$, $I_1 = \{2g-2+i, i, g+i, i, i+1\}$ and $I_2 = \{1, \ldots, 3g-3\} \setminus I_1$. This concludes the proof of Proposition 3.2.

Before we prove unitarity of the representation of the mapping class group given by the invariants of graphs on Riemann surfaces we discuss some properties of two special $(r-1) \times (r-1)$-matrices: the diagonal matrix A (see eq. (3.38))

$$
A_{ab} = \delta_{ab}\, q_a^2 \tag{3.52}
$$

and S^c (for fixed c) with matrix elements given by eq. (3.45)

$$
S^c_{ab} = \frac{q_a^{-2} q_b^{-2}}{w} \sum_d w_d^2 q_d^2 N_{ab}^{cd} \quad \text{where} \quad N_{ab}^{cd} = w_a w_b \begin{vmatrix} a & b & d \\ b & a & c \end{vmatrix}. \tag{3.53}
$$

This representation in terms of a 6j-symbol and the following relations are proved in Appendix B. Note that for $c = 0$ this formula coincides with the representation of S_{ab} (A.1) in [15] for the genus $g = 1$ case, ie. $S^0 = S$, because $N^{0d} = N^d$ is the fusion matrix (2.7). The matrix S^c is symmetric and $q_c^{-1/2} S^c$ is real

$$
S^c_{ab} = S^c_{ba} = q_c (S^c_{ab})^*. \tag{3.54}
$$

Moreover the matrices A and S^c are unitary

$$
A^\dagger A = 1, \quad S^c (S^c)^\dagger = 1^c. \tag{3.55}
$$

In the second relation 1^c has to be understood as the unit matrix with indices a subject to the condition $N_{aa}^c \neq 0$. We also have the relation[1]

$$AS^cAS^cA = \kappa S^c \quad \text{with} \quad \kappa = \frac{1}{w}\sum_d w_d^4 q_d^2 = q^{-3/2}\, e^{-i\pi(1/4+r/2)}. \tag{3.56}$$

The matrix N^{cd} (c and d fixed) with matrix elements N_{ab}^{cd} is diagonalized by S^c

$$(S^c)^{-1} N^{cd} S^c = \mathrm{diag}(S_{db}/S_{0b})_{b\in\mathcal{I}}. \tag{3.57}$$

The eigenvalues of N^{cd} are independent of c, which implies that N^{cd} is equivalent to the fusion matrix N^d

$$(S^cS^{-1})^{-1} N^{cd} S^c S^{-1} = N^d. \tag{3.58}$$

The unitarity of A and the symmetry of S^c are obvious, the other relations are proved in Appendix B.

By Proposition 3.1 we have now:

Theorem 3.3 *The representations of the mapping class group*

$$\varphi \mapsto \langle\, \underline{e}', \underline{\bar{f}}' \,|\, \pi(\varphi) \,|\, \underline{e}, \underline{\bar{f}} \,\rangle \tag{3.59}$$

on $V^{\Sigma g}$ (defined by eq. (3.32)) is unitary.

Proof: Since MCG^g is generated by $A_1, \ldots, A_g, A_{g+1}$ and $S_1, \ldots, S_g$ eqs. (3.55) imply unitarity because of eqs. (3.39) and (3.48), (3.50), (3.51) and transformations like (3.42).

Because of the decomposition formula of Proposition 3.2 we have moreover

Theorem 3.4 *The maps on $V_l^{\Sigma g}$ and $V_r^{\Sigma g}$, respectively,*

$$\varphi \;\mapsto\; \langle\, \underline{e}' \,|\, \pi_l(\varphi) \,|\, \underline{e} \,\rangle \tag{3.60}$$

$$\varphi \;\mapsto\; \langle\, \underline{\bar{f}}' \,|\, \pi_r(\varphi) \,|\, \underline{\bar{f}} \,\rangle \tag{3.61}$$

given by eqs. (3.35) - (3.37) define unitary ray representation of MCG^g such that $\pi = \pi_l \otimes \pi_r$ and $\pi_r = \pi_l^*$. For genus $g = 1$ the maps $\rho_l(\varphi)$ and $\rho_r(\varphi)$ given by

$$\rho_l(S) = \pi_l(S) \quad \text{and} \quad \rho_l(A) = \kappa^{-1/3}\pi_l(A) \tag{3.62}$$

for the generators and $\rho_r = \rho_l^*$ define representations of MCG^1.

Proof: It remains to prove that the relations for the generators of MCG^1 $S^4 = 1$ and $ASASA = S$ also hold for the representation matrices ρ_l. This follows from eqs. (3.55) - (3.54). Thus we have proved the main results of this section.

[1] The phase factor κ differs from that in [6] and [7] since we have a different sign convention for q_a^2.

Example 3.5 *(i) If $\varphi(A,S)$ is a word composed of A's and S's then*

$$\langle\, \underline{e}' \,|\, \pi_l(\varphi(A,S)) \,|\, \underline{e} \,\rangle = w^{N_S} \langle\, \underline{e}', \underline{0} \,|\, \pi(\varphi(A,S)) \,|\, \underline{e}, \underline{0} \,\rangle \tag{3.63}$$

where N_S is the number of S's in $\varphi(A,S)$.

(ii) For genus $g=1$ we have

$$\langle\, e' \,|\, \pi_l(A^{m_t}\, S\, A^{m_{t-1}}\, S \cdots A^{m_1}\, S) \,|\, e \,\rangle = (A^{m_t}\, S\, A^{m_{t-1}}\, S \cdots A^{m_1}\, S)_{e'e} \tag{3.64}$$

$$\langle\, e' \,|\, \pi_l(S\, A^{m_t}\, S\, A^{m_{t-1}}\, S \cdots A^{m_1}\, S) \,|\, e \,\rangle = (S\, A^{m_t}\, S\, A^{m_{t-1}}\, S \cdots A^{m_1}\, S)_{e'e} \tag{3.65}$$

where the matrix A is given by eq. (3.52) and S given by eq. (3.53) for $c=0$ is the Verlinde matrix $S_{ab} = (-1)^{2a+2b} \sin\frac{\pi}{r}(2a+1)(2b+1)/(w\,\sin\frac{\pi}{r})$.

4 Application to the partition function of arbitrary manifolds

Based on our discussion in Section 3 of the representation of the mapping class group, we now provide a formulation on how to calculate the Turaev-Viro state sum $Z(M)$ for an arbitrary oriented compact 3-manifold M. In particular we give an explicit formula for manifolds obtained from a figure-eight knot by an $(-n/m)$-surgery. Let M_Σ be an arbitrary handle body with boundary $\Sigma = \Sigma^g$, viewed as embedded in S^3. We set $\tilde{M}^*_\Sigma = S^3 \setminus M_\Sigma$ with $\partial \tilde{M}_\Sigma = \Sigma$, such that $\tilde{M}^*_\Sigma \cup_\Sigma M_\Sigma = S^3$. Let φ be an arbitrary orientation preserving diffeomorphism and set $M = \tilde{M}^*_\Sigma \cup_{(\Sigma,\varphi)} M_\Sigma$. It is well known that any 3-manifold can be obtained nonuniquely in this way [27]. By our previous discussion we may write the Turaev-Viro invariant of the 3-manifold M as

$$Z(M,r) = \langle\, \tilde{M}_\Sigma \,|\, \pi(\varphi) \,|\, M_\Sigma \,\rangle = \sum_{\underline{e},\underline{\bar{f}}} \langle\, \tilde{M}_\Sigma \,|\, \underline{e}, \underline{\bar{f}} \,\rangle \langle\, \underline{e}, \underline{\bar{f}} \,|\, \pi(\varphi) \,|\, M_\Sigma \,\rangle. \tag{4.66}$$

In particular we have for $\varphi = 1$ of course

$$Z(S^3,r) = \langle\, \tilde{M}_\Sigma \,|\, M_\Sigma \,\rangle = \langle\, \tilde{M}_\Sigma \,|\, \underline{0}, \underline{0} \,\rangle \langle\, \underline{0}, \underline{0} \,|\, M_\Sigma \,\rangle = w^{-2}. \tag{4.67}$$

Because of eq. (2.27) this means that $\langle\, \underline{0}, \underline{0} \,|\, M_\Sigma \,\rangle = w^{g-1}$ and $\langle\, \tilde{M}_\Sigma \,|\, \underline{0}, \underline{0} \,\rangle = w^{-g-1}$. We want to factorize the right hand side of eq. (4.66) into a left and a right handed contribution. The factorization of the first factor

$$\langle\, \tilde{M}_\Sigma \,|\, \underline{e}, \underline{\bar{f}} \,\rangle = w^{g+1} \langle\, \tilde{M}_\Sigma \,|\, \underline{e}, \underline{0} \,\rangle \langle\, \tilde{M}_\Sigma \,|\, \underline{0}, \underline{\bar{f}} \,\rangle = w^{g+1} \langle\, \tilde{M}_\Sigma \,|\, \underline{e} \,\rangle \langle\, \tilde{M}_\Sigma \,|\, \underline{\bar{f}} \,\rangle \tag{4.68}$$

follows from the trivial braiding of left and right handed lines proved in [15], which implies that the graphs $\mathcal{G}^{\Sigma}_{\underline{e}}$ and $\mathcal{G}^{\Sigma}_{\underline{\bar{f}}}$ may be moved in two nonintersecting balls $D^3 \subset S^3$, respectively. The normalization follows from the definitions (2.24), $Z(S^3) = w^{-2}$ and $\langle\, \tilde{M}_\Sigma \,|\, \underline{0}, \underline{0} \,\rangle = w^{1-g} \langle\, \tilde{M}_\Sigma \,|\, M_\Sigma \,\rangle = w^{-1-g}$. We have introduced $\langle\, \tilde{M}_\Sigma \,|\, \underline{e} \,\rangle = \langle\, \tilde{M}_\Sigma \,|\, \underline{e}, \underline{0} \,\rangle$ such that $\langle\, \tilde{M}_\Sigma \,|\, \underline{0} \,\rangle = w^{-g-1}$. The factorization of the second factor

$$\langle\, \underline{e}, \underline{\bar{f}} \,|\, \pi(\varphi) \,|\, M_\Sigma \,\rangle = w^{g-1} \langle\, \underline{e} \,|\, \pi_l(\varphi) \,|\, \underline{0} \,\rangle \langle\, \underline{\bar{f}} \,|\, \pi_r(\varphi) \,|\, \underline{0} \,\rangle \tag{4.69}$$

follows from Proposition 3.2 and eq. (2.27). Therefore we have

$$Z(M, r) = Z_l(M, r) \cdot Z_r(M, r) \tag{4.70}$$

where

$$Z_l(M, r) = e^{i\psi(\tilde{M}_\Sigma, \varphi)}\, w^g \sum_{\underline{e}} \langle\, \tilde{M}_\Sigma \,|\, \underline{e} \,\rangle \langle\, \underline{e} \,|\, \pi_l(\varphi) \,|\, \underline{0} \,\rangle \tag{4.71}$$

and $Z_r(M, r) = Z_l^*(M, r)$. For $\varphi = 1$ we have (compare eq. (4.67))

$$Z_l(S^3, r) = e^{i\psi}\, w^{-1}. \tag{4.72}$$

The phase $\psi(\tilde{M}_\Sigma, \varphi)$, which is of course not determined by the Turaev-Viro invariant, has to be chosen such that $Z_l(M, r)$ is invariant (see below).

We now discuss the case where Σ is a set of (possibly knotted) tori: $\Sigma = \bigcup_{i=1}^{N} (S^1 \times S^1)_i$ forming a link $\mathcal{L}$ with N components. For simplicity we write $\langle\, \tilde{M}_\Sigma \,| \,= \langle\, \mathcal{L} \,|$ and use $|\, M_\Sigma \,\rangle = |\, \underline{0}, \underline{0} \,\rangle$. The mapping class group of a torus is generated by the elements S and A with the relations $S^4 = \mathbf{1}$ and $(SA)^3 = S^2$. We use the representation as given in [15] and Theorem 3.4 (see also [18]). If we consider the map $\varphi = A_1^{n_1} \cdots A_N^{n_N} S_1 \cdots S_N$, then instead of the invariant (4.71) we get the formula of the following theorem due to Reshetikhin and Turaev [6].

Theorem 4.1 *Let $\mathcal{L}$ be a link of N components and framing $n_1, \ldots, n_N$ then*

$$Z_l(M, r) = \kappa^{-\sigma_\mathcal{L}}\, w^{1-N} \sum_{\underline{e}} \langle\, \mathcal{L} \,|\, \pi_l(A_1^{n_1} \cdots A_N^{n_N}) \,|\, \underline{e} \,\rangle w_{e_1}^2 \cdots w_{e_N}^2. \tag{4.73}$$

is invariant under Kirby moves, if the phase factor $\kappa = q^{-3/2} e^{-i\pi(1/4 + r/2)}$ is given by eq. (3.56) and $\sigma_\mathcal{L}$ is the signature of the linking matrix. Therefore $Z_l(M, r)$ is an invariant of the 3-manifold obtained by surgery along $\mathcal{L}$.

Note that formula (4.73) for $N = 1$ is compatible with (4.71) for $g = 1$. In our formulation the proof of this theorem [6] (see also [7]) reads as follows.

Proof: Let $\mathcal{L}'$ be the link obtained by a Kirby move at a line of $\mathcal{L}$ of colour e. We use

Theorem 2.11 to write the invariant of the link $\mathcal{L}'$ embedded in S^3 as an invariant of a planar graph, apply formula (B.7) of Appendix B and use again Theorem 2.11 in the inverse direction to obtain

$$\sum_{e'} w_{e'}^2 \langle\, \mathcal{L}' \,|\, \pi_l(\varphi') \,|\, \underline{e}, e' \,\rangle \;=\; \sum_{e'} w_{e'}^2 \, Z \left(\right.$$

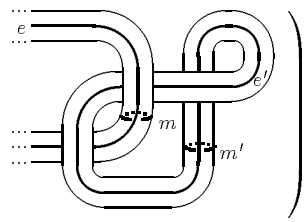

$$\left. \right)$$

$$= \; w^{\chi-2} \sum_{e'} w_{e'}^2 \, Z \left(\right.$$

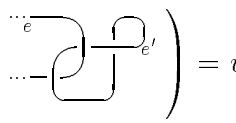

$$\left. \right) = w^{\chi-2} \, w \, \kappa \, Z \left(\right.$$

$$\left. \right)$$

$$= \; w \, \kappa \, Z \left(\right.$$

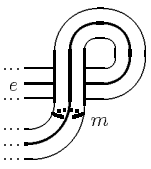

$$\left. \right) = w \, \kappa \, \langle\, \mathcal{L} \,|\, \pi_l(\varphi) \,|\, \underline{e} \,\rangle .$$

This relation also explains the local meaning of $\mathcal{L}$ and $\mathcal{L}'$. The normalization of eq. (4.73) is consistent with $\langle\, \mathcal{L} \,|\, \pi_l(A_1^{n_1} \cdots A_N^{n_N}) \,|\, \underline{0}, \underline{0} \,\rangle = \langle\, \mathcal{L} \,|\, \underline{0}, \underline{0} \,\rangle = w^{-2}$ and $\langle\, \underline{e} \,|\, \pi_l(S_1 \cdots S_N) \,|\, \underline{0} \,\rangle = S_{e_1 0} \cdots S_{e_N 0} = w^{-N} w_{e_1}^2 \cdots w_{e_N}^2$.

Invariance under Kirby moves obviously does not uniquely determine the phase factor in eq. (4.73). In Section 5 we present for special cases an "experimentally" obtained choice of the phase factor $\exp i\psi$ such that $Z_l(M,r)$ fits asymptotically for $r \to \infty$ with the asymptotic expansion of Witten's Chern-Simons functional integral $Z_{CS}(M,k)$ for $k = r + 2 \to \infty$. This choice of the phase does not agree with that of eq. (4.73). Formula (4.73) yield up to a factor w the Reshetikhin-Turaev [6] invariant of 3-manifolds in the slightly modified version of Kirby and Melvin [7] (see also [28])

$$Z_l(M,r) = w^{-1} \, \tau_r(M). \tag{4.74}$$

The matrix element $\langle\, \mathcal{L} \,|\, A_1^{n_1} \cdots A_N^{n_N} \,|\, \underline{e} \,\rangle$ in eq. (4.73) is the invariant of the link $\mathcal{L}$ with framings $n_1, \ldots, n_N$ of the components as given by formulas eq. (2.11) and eq. (2.12) for left handed lines with colours $\underline{e} = (e_1, \ldots, e_N)$. In particular for a single ($N = 1$) unknotted circle and framing $n = \pm 1$ eq. (4.73) yields by eqs. (2.12) and (3.38) (see also Fig. 7) the invariant of S^3

$$Z_l(S^3,r) = \kappa^{\mp 1} \sum_e \langle\, \mathcal{L} \,|\, \pi_l(A^{\pm 1}) \,|\, e \,\rangle w_e^2 = \kappa^{\mp 1} \, w^{-2} \sum_e w_e^4 \, q_e^{\pm 2} = w^{-1}. \tag{4.75}$$

This means invariance of $Z_l(M,r)$ under Kirby moves for this case.

We now return to eq. (4.71) and restrict attention to the case where Σ is a (possibly knotted) single torus $S^1 \times S^1$ forming a knot $\mathcal{K}$ of one component.

$$Z_l(M,r) = e^{i\psi}\, w \sum_e \langle\, \mathcal{K} \,|\, e \,\rangle \langle\, e \,|\, \pi_l(\varphi) \,|\, 0 \,\rangle \tag{4.76}$$

Relation (4.76) is the desired formula. The general case for the map φ belongs to a $-n/m$-surgery. We distinguish two cases

(i) $|n/m| > 1$ $(m \neq 0)$ Then we write n/m as a finite continued fraction expansion

$$\frac{n}{m} = m_t - \frac{1}{m_{t-1} - \frac{1}{\cdots - \frac{1}{m_1}}} \quad (1 \leq t < \infty, \quad m_i \geq 2)$$

with integers $m_1, \ldots, m_t$. The mapping class group element is then of the form

$$\varphi^{(-\frac{n}{m})} = A^{m_t}\, S\, A^{m_{t-1}}\, S \cdots A^{m_1}\, S. \tag{4.77}$$

and the matrix element in eq. (4.76) is given by the matrix product

$$\langle\, e \,|\, \pi_l(\varphi^{(-\frac{n}{m})}) \,|\, 0 \,\rangle = (A^{m_t}\, S \cdots A^{m_1}\, S)_{e0} \tag{4.78}$$

where A is the diagonal matrix of eq. (3.52) with diagonal elements q_a^2 and S is the matrix of eq. (3.53) for $c = 0$ which is the Verlinde matrix
$S_{ab} = (-1)^{2a+2b} \sin\frac{\pi}{r}(2a+1)(2b+1)/(w\, \sin\frac{\pi}{r})$.

(ii) $|n/m| < 1$ $(m \neq 0)$: Then we write

$$\frac{m}{n} = m_t - \frac{1}{m_{t-1} - \frac{1}{\cdots - \frac{1}{m_1}}} \quad (1 \leq t < \infty, \quad m_i \geq 2).$$

The mapping class group element is then of the form

$$\varphi^{(-\frac{n}{m})} = S\, A^{m_t}\, S\, A^{m_{t-1}}\, S \cdots A^{m_1}\, S. \tag{4.79}$$

and the matrix element in eq. (4.76) is given by the matrix product

$$\langle\, e \,|\, \pi_l(\varphi^{(-\frac{n}{m})}) \,|\, 0 \,\rangle = (S\, A^{m_t}\, S \cdots A^{m_1}\, S)_{e0}. \tag{4.80}$$

We obtain in particular

$$\langle\, e \,|\, \pi_l(\varphi^{(-\frac{n}{1})}) \,|\, 0 \,\rangle = q_e^{2n}\, S_{e0} = w^{-1} q_e^{2n}\, w_e^2 \tag{4.81}$$

$$\langle\, e \,|\, \pi_l(\varphi^{(-\frac{1}{m})}) \,|\, 0 \,\rangle = \sum_{e'} S_{ee'} q_{e'}^{-2m}\, S_{e'0}. \tag{4.82}$$

What remains is to calculate the coefficients $\langle\, \mathcal{K} \,|\, e \,\rangle$ depending on the way $\mathcal{K}$ is embedded in S^3. They are invariants of knots. Assume now in addition that $\mathcal{K}$ is a figure-eight knot.

Lemma 4.2 *If $\mathcal{K}$ is the figure-eight knot, then*

$$\langle\, \mathcal{K} \,|\, e \,\rangle = w^{-2} \sum_{b,c} w_b^2 w_c^2 q_b^2 q_c^{-2} \begin{vmatrix} e & e & b \\ e & e & c \end{vmatrix} \tag{4.83}$$

Proof: We use Theorem 2.11 to write the invariant of the knot embedded in S^3 as an invariant of a planar graph

$\langle\, \mathcal{K} \,|\, e \,\rangle \;=\; Z\Big($ 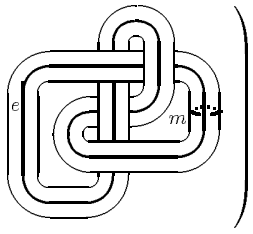 $\Big) = w^{-2}\, Z\Big($ 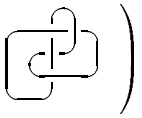 $\Big)$

$= w^{-2} \sum_{b,c} w_b^2 w_c^2\, Z\Big($ 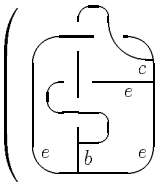 $\Big) = w^{-2} \sum_{b,c} w_b^2 w_c^2 q_b^2 q_c^{-2}\, Z\Big($ 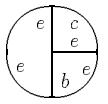 $\Big)$.

The completeness and Racah relations (B.1) have been used. By eq. (2.8) we obtain eq. (4.83).

Corollary 4.3 *For the figure-eight knot and a $(-n/m)$ surgery the resulting manifold $M_8(-n/m)$ has a Turaev-Viro state sum $Z(M_8(-n/m))$ equals $|Z_l(M_8(-n/m))|^2$ with*

$$Z_l(M_8(-n/m), r) = e^{i\psi}\, w^{-1} \sum_{b,c,e} w_b^2 w_c^2 q_b^2 q_c^{-2} \begin{vmatrix} e & e & b \\ e & e & c \end{vmatrix} \langle\, e \,|\, \pi_l(\varphi^{(-\frac{n}{m})}) \,|\, 0 \,\rangle. \tag{4.84}$$

Example 4.4 *We may write eq. (4.76) also as*

$$Z_l(M, r) = e^{i\psi}\, w^{-1} \sum_e \langle\, \mathcal{K} \,|\, \pi_l(\hat{\varphi}) \,|\, e \,\rangle \langle\, e \,|\, \pi_l(S) \,|\, 0 \,\rangle \tag{4.85}$$

with $\varphi = \hat{\varphi}\, S$. For a $(-2/1)$- surgery at a figure-eight knot

$$\langle\, \mathcal{K} \,|\, \pi_l(A^2) \,|\, e \,\rangle = Z\Big($ 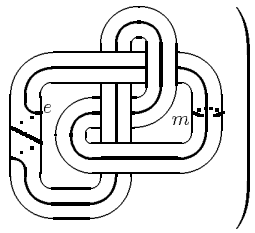 $\Big)$.

The meridian m undercrosses the line with colour e such that it is left handed. For a $(-1/2)$- surgery at a figure-eight knot

$$\langle\, \mathcal{K} \,|\, \pi_l(S\, A^{-2}) \,|\, e \,\rangle = Z \left(\right.$$
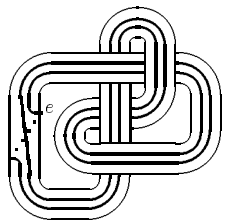

$$\left. \right) .$$

For simplicity we have not drawn the image of the meridian.

5 Numerical results

We have analyzed numerically the partition function $Z(M_8(-n/m), r)$ given by eqs. (4.81)-(4.84) for several cases. For this we used the explicit formula for the 6j-symbol taken from [29] with the following identification

$$\begin{vmatrix} a & b & e \\ d & c & f \end{vmatrix} = i^{-2(a+b+c+d+e+f)} \begin{Bmatrix} a & b & e \\ d & c & f \end{Bmatrix}^{RW} \tag{5.86}$$

where the right hand side is the quantity defined in [29], Theorem 5.1 as

$$\begin{aligned} \begin{Bmatrix} a & b & e \\ d & c & f \end{Bmatrix}^{RW} &= \triangle(abe)\triangle(acf)\triangle(cde)\triangle(dbf) \\ &\quad \times \sum_z (-1)^z [z+1]_q! \Big\{ [z-a-b-e]_q! [z-a-c-f]_q! \\ &\quad \times [z-b-d-f]_q! [z-d-c-e]_q! [a+b+c+d-z]_q! \\ &\quad \times [a+d+e+f-z]_q! [b+c+e+f-z]_q! \Big\}^{-1} \end{aligned} \tag{5.87}$$

with (see [15], rel. (3.6))

$$\triangle(abc) = \left\{ \frac{[-a+b+c]_q! [a-b+c]_q! [a+b-c]_q!}{[a+b+c+1]_q!} \right\}^{\frac{1}{2}} \tag{5.88}$$

The sum in (5.87) is taken over all nonnegative integers z with nonnegative arguments in the square brackets. Also

$$[n]_q! = 1_q 2_q \cdots n_q, \quad \text{with} \quad n_q = \frac{q^n - q^{-n}}{q - q^{-1}}. \tag{5.89}$$

(Note that the $q^{1/2}$ of Kirillov and Reshetikin [29] is our q and the q_0 of Turaev and Viro [8]).

The numerical calculations were performed for various manifolds $M_8(-n/m)$ and values of r in the range $4 \leq r \leq 403$. We used a Fortran program with double precision. Note that due to eqs. (4.83) and (5.86) - (5.88) the numerical calculation is essentially a four loop calculation such that $Z_l(M_8(-n/m), r)$ is a sum of $\approx r^4$ contributions with a corresponding computing time behaviour. This was the reason that for values of r above $r \approx 440$ the results tended become unreliable in double precision. It is possible to extend the range of r up to ~ 500 by working with G-precision. Here, however, we shall only report on results in the range given above. The absolute values of $Z_l(M_8(-n/m), r)$ turn out to be all of order one in contrast to the case of lens spaces (see eg. [19][20]).

Example 5.1 *Fig. 12a plots the values $Z_l(M_8(-6/1), r)$ for even $r = 4, \ldots, 403$ as dots in the complex plane. The phase in eq. (4.84) is taken as $\psi = \pi r$ (see eq. (5.95) below). It turns out that for odd r these invariants are zero (see below and Appendices C and D). Note that $M_8(-6/1)$ is a hyperbolic manifold.*

Example 5.2 *Fig. 12b plots the values $Z_l(M_8(-1/6), r)$ for $r = 4, \ldots, 403$ as dots in the complex plane. The phase in eq. (4.84) for $m = 1$ is taken as $\psi = 0$ (see eq. (5.100) below).*

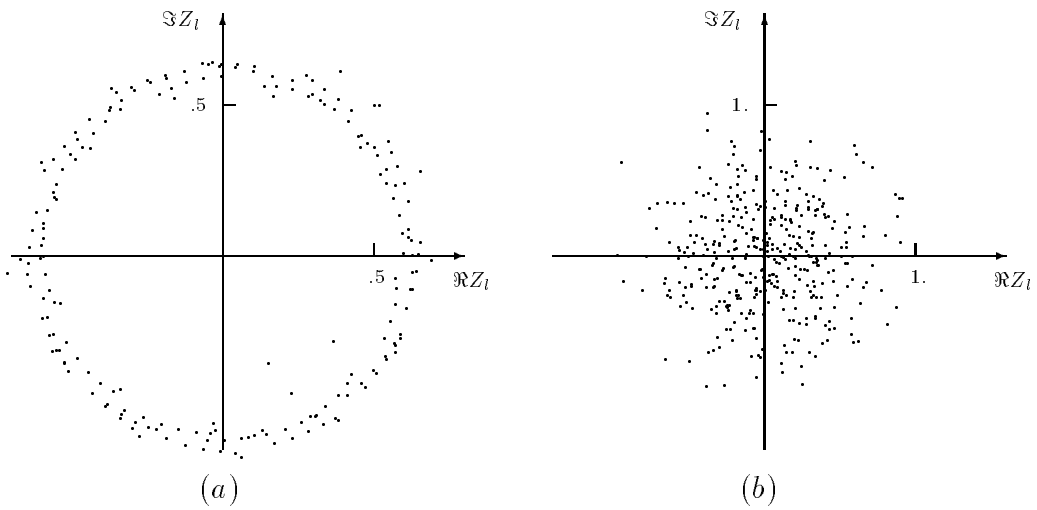

Figure 12: *The values of (a) $Z_l(M_8(-6/1), r)$ and (b) $Z_l(M_8(-1/6), r)$ $(4 \leq r \leq 403)$*

The main interest of our analysis was to see whether the semiclassical analysis $r \to \infty$ could be correct. Recall that by eq. (1.1) (see also (4.77) and (4.84)) $Z_l(M_8(-n/m), r)$ and $Z_{CS}(M_8(-n/m), k = r - 2)$ should agree up to a phase. Now the semiclassical conjecture is that (see [19]) for large r

$$Z_{CS}(M, k = r - 2) \cong \frac{1}{2} \sum_{A \ flat} C_A \, r^{-\frac{1}{2} \dim H^0(A)} \cdot e^{2\pi i r S_{CS}(A)}, \tag{5.90}$$

if all flat connections are isolated (modulo gauge transformations) such that in particular $\dim H^1(A) = 0$ there. This is indeed the case for all examples we have considered. Therefore the leading contributions in eq. (5.90) arise from the irreducible flat bundles, where $H^0(A) = 0$. Since the structure group is $SU(2)$ and since we consider the adjoint representation, $\dim H^0(A)$ can only take the values 0 (irreducible case), 1 (reducible to $U(1)$) or 3 (the trivial case with $S_{CS}(A) = 0$). Finally, up to a phase C_A^2 is conjectured to be the corresponding Ray-Singer torsion (see e.g. [19]). To see whether (5.90) holds we

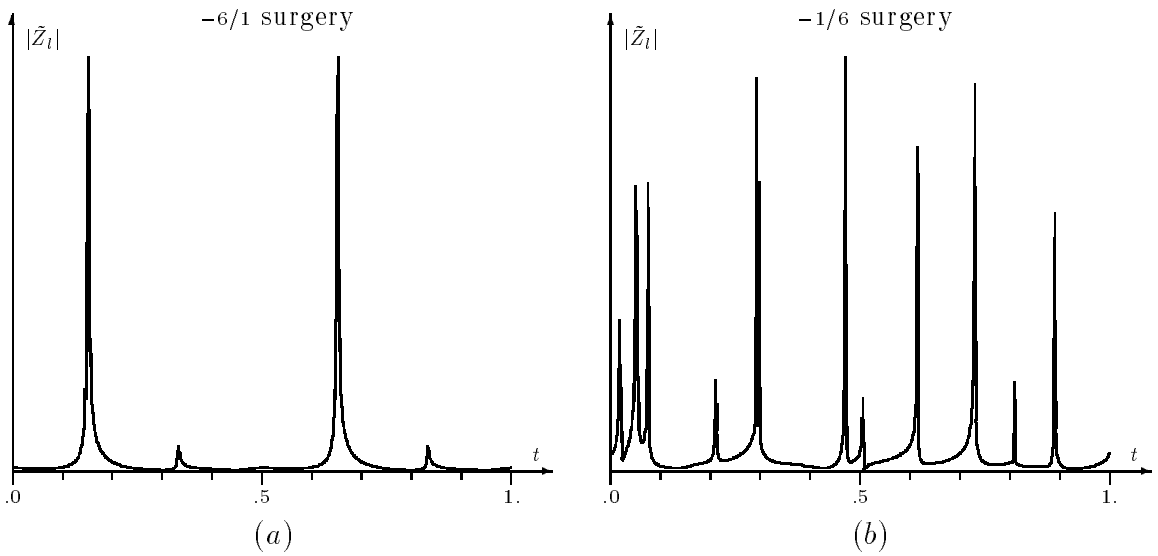

Figure 13: *The Fourier transforms (a):* $|\tilde{Z}_l(M_8(-6/1), t)|$ *and (b):* $|\tilde{Z}_l(M_8(-1/6), t)|$ *for* $(0 \leq t \leq 1)$.

performed a Fourier transform

$$\tilde{Z}_l(M_8(-n/m), t) = \frac{1}{400} \sum_{r=4}^{403} Z_l(M_8(-n/m), r)\, e^{-2\pi i t r}, \quad 0 \leq t \leq 1. \tag{5.91}$$

This function should show prominent maxima at values of t which correspond to $S_{CS}(A)$ for flat A. In principle the absolute values of the C_A's may be determined from $|\tilde{Z}_l(M, t)|$ at the maxima unless there are two or more different flat connections with the same Chern-Simons action and the same $\dim H^0(A)$. This is for example the case for $M_8(-n/1)$ with $n = 8, 16, 20$ (see Appendix C).

Example 5.3 *Fig. 13a plots the absolute value of the Fourier transform* $\tilde{Z}_l(M_8(-6/1), t)$ *where the phase in eq. (4.84) for* $m = 1$ *has be taken as* $\psi = \pi r$ *(see eq. (5.95) below). The function has a period of* $t = 1/2$ *since* $Z_l(M_8(-6/1), r)$ *vanishes for odd* r. *We interpret*

the big peaks to correspond to the leading contributions of the asymptotic expansion (5.90) with $\dim H^0(A) = 0$ *and the small ones to* $\dim H^0(A) = 1$.

Example 5.4 *Fig. 13b plots the absolute value of the Fourier transform* $\tilde{Z}_l(M_8(-1/6), t)$ *where the phase in eq. (4.84) has be taken as* $\psi = 0$ *(see eq. (5.100) below).*

To locate the maxima of $|\tilde{Z}_l(M_8(-n/m), t)|$, we also employed the following procedure. We considered the set of points

$$Z_l(M_8(-n/m), r, t) = Z_l(M_8(-n/m), r)\, e^{-2\pi i t r} \tag{5.92}$$

For t at a maximum these members typically arrange in a symmetric fashion. Fig. 14 provides two examples at the maxima a) $t = 0.15127$ b) $t = 0.33333$ for the manifold $M_8(-1/6)$ (compare Fig. 13 and Tables 1 and 2). Note that Fig. 12a correspond to the choice $t = 0$. In all the examples considered, this procedure allowed for an evaluation of

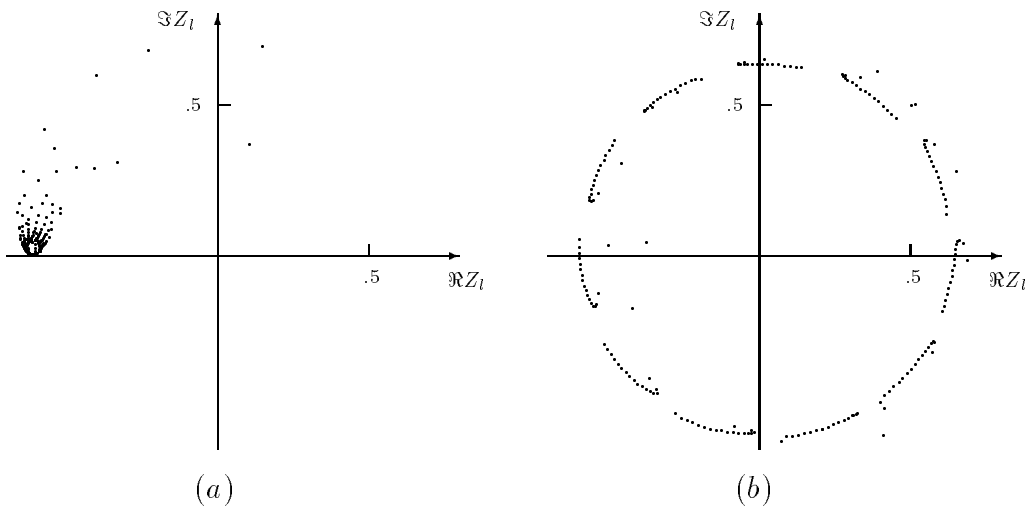

Figure 14: *The values of* $Z_l(M_8(-6/1), r)\, e^{-2\pi i t r}$ *: (a)* $t = .15127$ *and (b)* $t = .33333$.

the maxima up to 6 digits. Since Z_{CS} and Z_l might differ by a phase factor, the differences in the maxima should correspond to the differences in the Chern-Simons invariants of flat bundles.

Now Kirk and Klassen [2] describe explicitly how to obtain all reducible and irreducible flat connections up to gauge equivalence of $M_8(n/m)$ and give precise formulae for computing the corresponding Chern-Simons invariants. For the convenience of the reader we briefly recall these results in Appendix C where we also derive some consequences from these formulae. The set of Chern-Simons invariants of $M_8(n/m)$ corresponding to

reducible flat connections is given by

$$\left\{ -\frac{t^2 p}{n} \;\Big|\; t = 0, 1, \ldots, \left[\frac{n}{2}\right] \right\}, \tag{5.93}$$

where p is an integer such that $p \cdot m \equiv -1 \; mod \; n$ (see Appendix C). In our numerical analysis the reducible flat connections show up as small peaks (see e.g. Example 5.3, Fig. 13a and Table 1). This is obviously due to the fact that these contributions in formula (5.90) go like $r^{-1/2}$. Comparing these values (5.93) with the values obtained from our numerical calculations starting from eq. (4.84), we can determine (at least asymptotically for $r \to \infty$) the phase ψ in eqs. (4.71) and (4.84), which is undetermined from the Turaev-Viro invariants. It turns out that for all examples of 3-manifolds $M_8(-n/m)$ we have considered the phase is consistent with

$$\psi(n, m, r) = \frac{\pi}{2} K(n, m) r \qquad \text{with} \quad K(n, m) \in \mathbf{Z}_4 \tag{5.94}$$

at least asymptotically for large r.

Table 1: The values of $S_{CS}(A)$ for examples of reducible representations for $(-n/1)$ surgery

surgery	# red. reps	K	S_{CS} by (4.84)	S_{CS} by [2]	S_{CS} by (4.84)	S_{CS} by [2]
-3/1	1	3	0.66681	2/3		
-4/1	1	0	0.75000	3/4		
-5/1	2	1	0.19997	1/5	0.79999	4/5
-6/1	3	2	0.3333	1/3	0.83333	5/6
			0.5012	1/2		

In Table 1 we list for some examples the number $K(n, m)$ and the values of S_{CS} obtained by our numerical method compared with the values obtained by the method of Kirk and Klassen [2].

In [2] Kirk and Klassen provide for the examples $(n/m) = (-3/1), (-1/1), (-1/2), (-1/3)$ a list of all irreducible representations of $\pi_1 M_8(n/m)$ and the corresponding Chern-Simons invariants. With the techniques presented in Appendix C we have extended their list by more examples to compare the values of $S_{CS}(A)$ predicted by the semiclassical approximation formula (5.86) with the actual values given by eqs. (C.4,C.5). To find the solutions of (C.3) and to calculate the corresponding values of eqs. (C.4,C.5) we used *Mathematica*.

Some of the results are listed in Tables 2-4. They also show excellent agreement between the two methods. The following comments are also based on an analysis of examples not listed in our tables.

Table 2: The values of $S_{CS}(A)$ for examples of $(-n/1)$-surgery for irreducible representations

surgery	# irr. reps	K	S_{CS} by (4.84)	S_{CS} by [2]	S_{CS} by (4.84)	S_{CS} by [2]
-0/1	0	3	0.00000	0.0	0.20000	0.2
			0.80000	0.8		
-1/1	2	1	0.27978	0.279762	0.85116	0.8511905
-2/1	2	2	0.387512	0.3875	0.88750	0.8875
-3/1	2	3	0.479178	0.479166	0.91667	0.91666
-4/1	2	0	0.55019	0.55	0.950009	0.95
-5/1	2	1	0.054478	0.054458	0.605920	0.6059135
-6/1	2	2	0.151275	0.151265	0.651283	0.651265
-8/1	3	0	0.29997	0.3	0.70003	0.7
			0.721091	0.721304		
-12/1	4	0	0.050089	0.05	0.489647	0.4896907
			0.489647	0.4896907	0.450186	0.45
-14/1	6	2	0.048320	0.0485379	0.055263	0.054853
			0.161499	0.1614793	0.548319	0.5485379
			0.555265	0.554853	0.661497	0.6614793
-16/1	4	0	0.200064	0.2	0.251354	0.251307
			0.799979	0.8		
-18/1	6	2	0.306522	0.3064713	0.325624	0.3255013
			0.413818	0.413881	0.806520	0.8064713
			0.825627	0.8255013	0.913822	0.913881

a) For $(-n/1)$-surgery (compare Table 2) the phase factor in eq. (4.84) turns out to be consistent with the choice

$$e^{i\psi} = e^{i\pi\, nr/2}\ , \quad \text{i.e. } K(n,1) = n \tag{5.95}$$

(at least asymptotically for large r). Note that this phase factor is an invariant of the 3-manifold $M_8(-n/1)$. This is because the Reshetikhin-Turaev [6] invariant of 3-manifolds in the slightly modified version of Kirby and Melvin [7] $\tau_r(M)$ (see eqs. (4.74)) for $r = 3$ takes the values

$$\tau_3(M_8(-n/1)) = \kappa\, \frac{1}{\sqrt{2}}\, \left(1 + e^{-i\pi\, n/2}\right). \tag{5.96}$$

This result is obtained as follows. For $r = 3$ in eq. (4.84) only $b = c = 0$ and $e = 0, 1/2$ contribute. Therefore with eq. (4.81) we have

$$Z_l(M_8(-n/1), 3) = e^{i\psi}\, w^{-2} \sum_{e=0}^{1/2} w_e^2\ q_e^{2n} \begin{vmatrix} e & e & 0 \\ e & e & 0 \end{vmatrix}. \tag{5.97}$$

Now by eqs. (2.6), (2.9) and (2.13) $w_0^2 = 1$, $w_{1/2}^2 = -1$, $q_0 = 1$, $q_{1/2} = -q^{3/2} =$

$e^{-i\pi/2}$, $w^2 = 2$ and $\begin{vmatrix} 0 & 0 & 0 \\ 0 & 0 & 0 \end{vmatrix} = 1$, $\begin{vmatrix} 1/2 & 1/2 & 0 \\ 1/2 & 1/2 & 0 \end{vmatrix} = -1$ (see e.g. [8]) giving

$$Z_l(M_8(-n/1), 3) = e^{i\psi}\frac{1}{2}\left(1 + e^{-i\pi\, n/2}\right). \tag{5.98}$$

In particular for $n = 4n' + 2$ this vanishes. As already stated, the big peaks in the function $\tilde{Z}_l(M, t)$ (compare e.g. Fig. 13 for $n = 6$) correspond to the leading contributions of the asymptotic expansion (5.90) with $\dim H^0(A) = 0$ and the small ones to $\dim H^0(A) = 1$.

aa) For $m = 1$ and $n > 4$, in which case the space $M_8(-n/m)$ is hyperbolic, there is at least one flat $SU(2)$-connection A with vanishing cohomology. For increasing n there is a proliferation in the number of such flat connections (modulo gauge equivalence) (see the remarks after eq. (C.3) in Appendix C).

ab) The numerical calculations confirm the analytic results (see Appendices C and D) that $Z_l(M_8(-n/1), r) = 0$ for all odd r in case $n \equiv 2\ mod\ 4$. The case $n = 6$ is depicted in Fig. 13a showing that $\tilde{Z}_l(M_8(-6/1), t)$ is indeed periodic in t with period $1/2$.

ac) For the exceptional case of $M_8(0/1)$, which for the case of an unknotted torus would correspond to $S^2 \times S^1$ we find the closed formula (guessed by our numerical results)

$$Z_l(M_8(0/1), r) = \frac{\cos 2\pi/5 - \cos 2\pi r/5}{2 \sin \pi/5\ \sin 2\pi/5} \tag{5.99}$$

In this case the semiclassical approximation is exact. This is analogous to the situation for lens spaces (see [20]). This result also agrees with the analytic result of Kirk and Klassen according to which there are two Chern-Simons invariants with values $\pm\frac{1}{5}$ (and vanishing cohomology) [2].

ad) For the case $n = 1, m = 1$ (the Seifert homology sphere $-\Sigma(2, 3, 7)$) we obtain two maxima for $|\tilde{Z}_l|$ located near

$$1 - \frac{25}{4 \cdot 42} \quad \text{and} \quad 1 - \frac{121}{4 \cdot 42}$$

This is compatible with the result of Kirk and Klassen giving two flat connections A_1 and A_2 with

$$S_{CS}(A_1) = -\frac{11^2}{4 \cdot 42} \quad \text{and} \quad S_{CS}(A_2) = -\frac{5^2}{4 \cdot 42}$$

ae) For $n = 3, m = 1$ (a Seifert fibered space over S^2 with Seifert invariants $(3,-2),\ (3,1),\ (4,1)$). Here Kirk and Klassen predict two values

$$S_{CS}(A_1) = -\frac{2^2}{4\cdot 12} \quad \text{and} \quad S_{CS}(A_2) = -\frac{5^2}{4\cdot 12}$$

We have found two strong maxima of $\tilde{Z}_l$ at $t_1 = 1-5^2/(4\cdot 12)$ and $t_2 = 1-2^2/(4\cdot 12)$ and a small maximum at $t_3 = 2/3$ if we take in eq. (5.94) the choice $K(3,1) = 3$ (see eq. (5.95)).

Table 3: The values of $S_{CS}(A)$ for examples of $(-1/m)$-surgery (for the case of $-1/8$ one spike at $S_{CS} = 0.17133$ is not visible because it is too close to that of $S_{CS} = 0.172535$)

surgery	# irr. reps	S_{CS} by (4.84)	S_{CS} by [2]	S_{CS} by (4.84)	S_{CS} by [2]
-1/2	4	0.053927	0.053933	0.235109	0.23516
		0.514125	0.514125	0.828180	0.828117
-1/6	12	0.018324	0.018451	0.051140	0.051163
		0.074568	0.07461	0.211492	0.21082
		0.291498	0.292507	0.298875	0.297362
		0.470291	0.470357	0.504663	0.504638
		0.614698	0.614739	0.729624	0.729587
		0.810647	0.810042	0.890340	0.890394
-1/8	16	0.003120	0.00348	0.086381	0.08637
		———	0.17133	0.172185	0.172535
		0.207460	0.20804	0.272334	0.272329
		0.400936	0.40089	0.415939	0.415986
		0.514109	0.51386	0.555343	0.55579
		0.593689	0.593654	0.720535	0.7205257
		0.808226	0.807600	0.850603	0.85053
		0.867921	0.868405	0.989921	0.990035

b) For $(-1/m)$-surgery (compare Table 3) the phase factor in eq. (4.84) turns out to be consistent with the choice (again at least asymptotically for large r)

$$e^{i\psi} = 1\ , \quad \text{i.e. } K(1,m) = 0 \tag{5.100}$$

and the numerical results are in agreement with the above observation that there are $2m$ irreducible flat connections (modulo gauge equivalence). Since the $M_8(-1/m)$ are homology spheres there are no nontrivial reducible representations.

c) **Example 5.5** *Fig. 15a plots the absolute value of the Fourier transform* $\tilde{Z}_l(M_8(-3/2), t)$ *and Fig. 15b that of* $\tilde{Z}_l(M_8(-2/3), t)$.

For all cases the maxima are at the same values as calculated using the methods of Kirk and Klassen ([2], p. 363), i.e. Z_l seems to agree with Z_{CS} in these cases which means that $K(2,3) = K(3,2) = 0$.

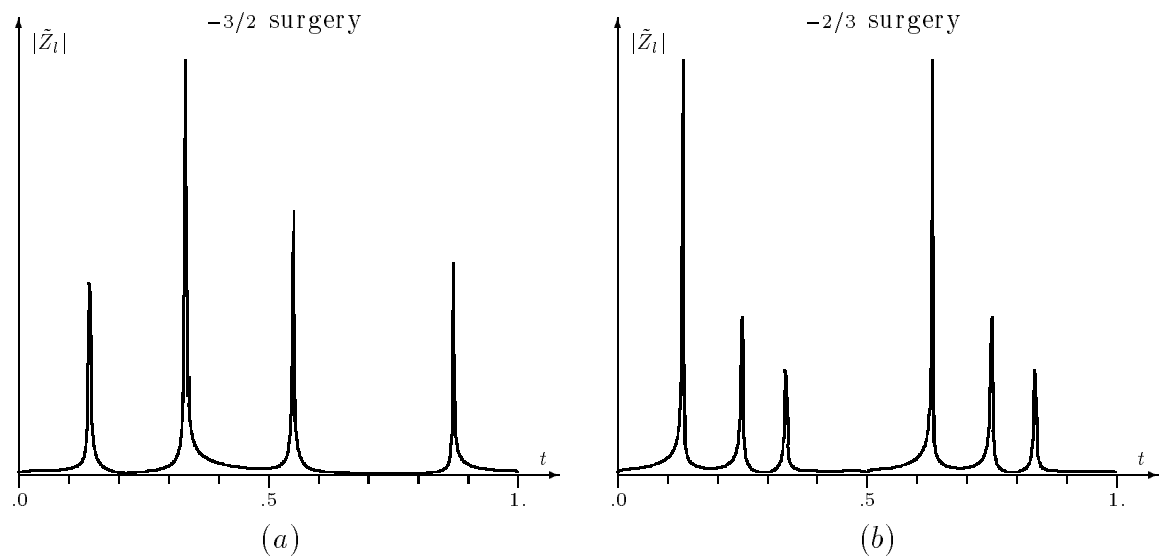

Figure 15: *The Fourier transforms (a):* $|\tilde{Z}_l(M_8(-3/2),t)|$ *and (b):* $|\tilde{Z}_l(M_8(-2/3),t)|$ *for* $(0 \leq t \leq 1)$.

Table 4: The values of $S_{CS}(A)$ for $(-3/2)$ and $(-2/3)$ surgery.

surgery	# irr. reps	K	S_{CS} by (4.84)	S_{CS} by [2]	S_{CS} by (4.84)	S_{CS} by [2]
-3/2	4	0	0.141068	0.141138	0.333369	0.333333
			0.548895	0.548930	0.870718	0.870641
-2/3	6	0	0.129545	0.129563	0.248862	0.248874
			0.336324	0.336288	0.629556	0.629563
			0.748850	0.748874	0.836311	0.836288

d) We have analyzed numerically the phase factor $e^{i\psi}$ for manifolds $M_8(-n/m)$ with $n > 0, m > 0, n/m > 1$ and for values of m from 2 up to 15. In total we have looked at about 400 manifolds. Our numerical results indicate the following rules: Asymptotically for large r the phase ψ is again of the form (5.94). In particular $K(n,m)$ is fixed only *mod* 2 if $Z_\ell(M_8(-n/m),r) = 0$ for r odd. Also $K(n,m)$ is quasiperiodic in n with quasiperiod $\pm m$, i.e. $K(n+m,m) \equiv K(n,m) \pm m$ *mod* 4 holds with a minus sign if $m \equiv 1$ *mod* 4 and a plus sign otherwise. We have not been able to find a general closed form for $K(n,m)$ as a function of n and m. In Table 5 we have listed the values of K for $m = 1,\ldots,12$ and some low values of $n > m$. For $m = 4$ we found $K(n,4) = 0$ for all $n > 4$.

To sum up, within our limits of numerical accuracy and for the examples considered we have been able to confirm the asymptotic expansion (5.90) up to contributions going like

Table 5: Values of $K(n,m)$ for different manifolds $M_8(-n/m)$.

n/m	0/1	1/1	2/1	3/1	4/1	5/1	6/1	7/1	8/1	9/1
K	0	1	2	3	0	1	2	3	0	1
n/m	3/2	5/2	7/2	9/2	11/2	13/2	15/2	17/2	19/2	21/2
K	0	2	0	2	0	2	0	2	0	2
n/m	4/3	5/3	7/3	8/13	10/3	11/3	13/3	14/3	16/3	17/3
K	0	2	3	1	2	0	1	3	0	2
n/m	6/5	7/5	8/5	9/5	11/5	12/5	13/5	14/5	16/5	17/5
K	2	3	2	2	1	2	1	1	0	1
n/m	7/6	11/6	13/6	17/6	19/6	23/6	25/6	29/6	31/6	35/6
K	0	0	2	2	0	0	2	2	0	0
n/m	8/7	9/7	10/7	11/7	12/7	13/7	15/7	16/7	17/7	18/7
K	0	0	2	2	0	2	3	3	1	1
n/m	9/8	11/8	13/8	15/8	17/8	19/8	21/8	23/8	25/8	27/8
K	0	2	1	0	0	2	1	0	0	2
n/m	10/9	11/9	13/9	14/9	16/9	17/9	19/9	20/9	22/9	23/9
K	2	1	1	2	2	2	1	0	0	1
n/m	11/10	13/10	17/10	19/10	21/10	23/10	27/10	29/10	31/10	33/10
K	0	0	0	0	2	2	2	2	0	0
n/m	12/11	13/11	14/11	15/11	16/11	17/11	18/11	19/11	20/11	21/11
K	0	2	0	1	0	2	2	3	0	2
n/m	13/12	17/12	19/12	23/12	25/12	29/12	31/12	35/12	37/12	41/12
K	0	0	2	0	0	0	2	0	0	0

$r^{-\frac{1}{2}}$, i.e. for irreducible flat connections the coefficient in front of $\exp 2\pi i r S_{CS}(A)$ behaves like a constant and for reducible ones with $\dim H^0(A) = 1$ like $r^{-\frac{1}{2}}$. In addition for some manifolds (like e.g. $n/m = 7/1, 16/1, 22/1$) we have found peaks whose amplitudes indicate at least an r^{-2} decay. To the best of our knowledge, so far such contributions to the semiclassical asymptotic expansion have no interpretation yet. The technique used to see the rate of decay was to modify eq. (5.91) by introducing the quantity

$$\begin{aligned}\tilde{Z}_\ell(M_8(-n/m), t; r_{min}, r_{max}, \alpha) \\ = \; (r_{max} - r_{min})^{-1} \sum_{r=r_{min}}^{r=r_{max}} r^\alpha Z_l(M_8(-n/m), r) e^{-2\pi i t r}\end{aligned}$$

such that $\tilde{Z}_\ell(M_8(-n/m), t) = \tilde{Z}_l(M_8(-n/m/, t; 4, 403, 0)$. We then looked at the absolute value of the peaks for varying r_{min}, r_{max} and α. Figures 16a-c provide an example for the case $n/m = 16/1$ for which $\exp i\psi = 1$ (see rel. (5.95)). Fig. 16a with $\alpha = 0$ shows that the amplitudes for the irreducible flat connections (indicated by arrows, see Table 2) stay constant for varying r_{max} and r_{min}. Fig. 16b with $\alpha = 1/2$ shows that the amplitudes of the reducible flat connections (again indicated by arrows, see Table 1) behave like $r^{-1/2}$.

Fig. 16c with $\alpha = 2$ indicates that the peak at 0.6104 (which is not the value for the Chern-Simons action of a flat connection) has an amplitude which decays at least like r^{-2}. In Figures 16b,c the peaks corresponding to irreducible flat connections have been cut off. Figures 16 also show that for $Z_l(M_8(-16/1, r))$ the asymptotic regime sets in at $r \approx 100$.

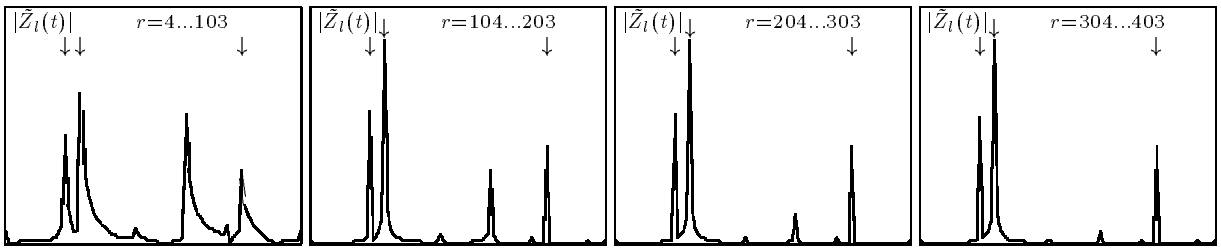

$(a): \quad \alpha = 0$

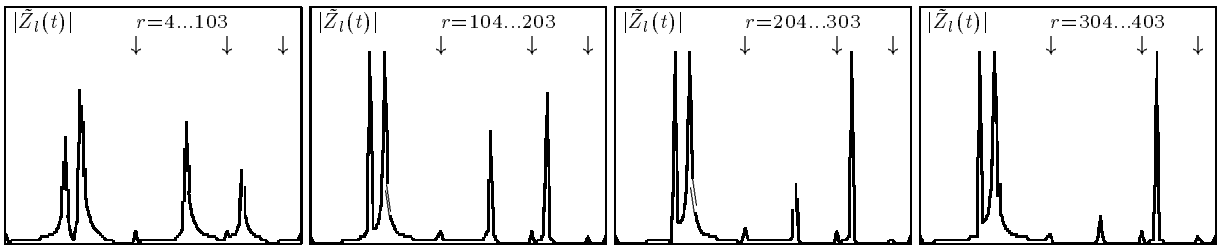

$(b): \quad \alpha = 1/2$

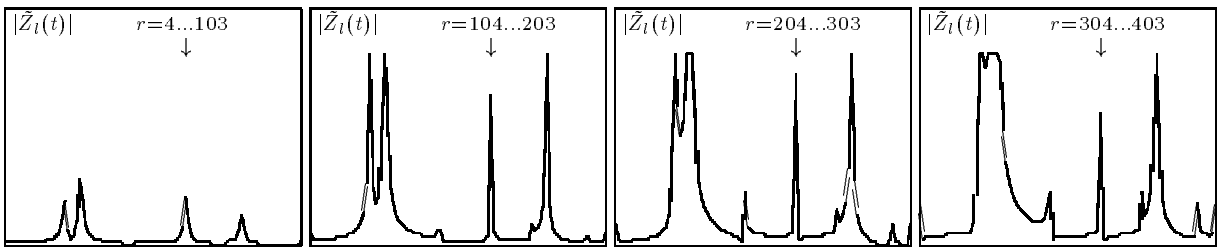

$(c): \quad \alpha = 2$

Figure 16: *The absolute value* $|\tilde{Z}_l(M_8(-16/1), t; r_{min}, r_{max})|$ *of the Fourier transform of* $r^\alpha Z_l(M_8(-16/1), r)$ *for some* r*-regimes.*

Appendix

A Proof of an orthogonality relation for the canonical graph of handle bodies

In this appendix we outline the proof of eq. (2.23). To this end we we cut the manifold (2.21)

$$(M^*_{\Sigma^g} \setminus \mathcal{T}_{\mathcal{G}^{\Sigma^g *}}) \underset{\Sigma^g}{\cup} (M_{\Sigma^g} \setminus \mathcal{T}_{\bar{\mathcal{G}}^{\Sigma^g}}) \cong \Sigma^g \times I \qquad (I = [0,1]) \tag{A.1}$$

into simple pieces. We consider a hollow cylindric part which is the neighbourhood of the lines with colours $e = e_i, \bar{f} = \bar{f}_i, e' = e'_i, \bar{f}' = \bar{f}'_i$ for some i, $(1 \leq i \leq 3g-3)$. We apply some results of [15] which are recalled in Section 2 and Appendix B: Lemma 2.10 how to introduce hollow tubes and Lemma 2.9 how to cut full cylinders. Using in addition eqs. (B.5) and (B.6) we have the following cutting rule

$Z\Bigg($ $\Bigg) = w^2 \, \frac{\delta_{ee'}\,\delta_{\bar{f}\bar{f}'}}{w_e^2\, w_{\bar{f}}^2}\, Z\Bigg($ 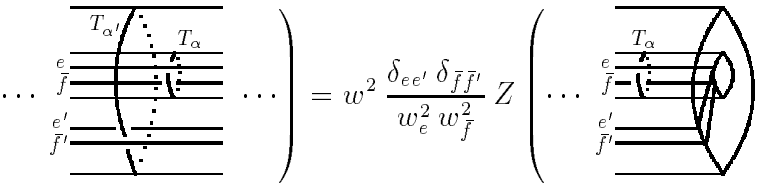 $+ \begin{matrix}\text{mirror-}\\ \text{image}\end{matrix} \cdots \Bigg).$ (A.2)

Applying this rule $3g-3$ $(g>1)$ times, the manifold (A.1) may be cut into $2g-2$ pieces of the form

$M(T_{\underline{\alpha}}) =$ 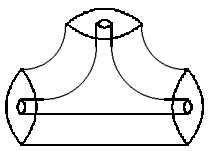 . (A.3)

These manifolds are equipped with graphs $|G|_{e_1 e_2 e_3 \bar{f}_1 \bar{f}_2 \bar{f}_2}$ where the e- and the $\bar{f}$-lines branch at a 3-vertex, respectively. In addition there are the meridians. Using again the cutting rules of [15] one finds

$$Z(M(T_{\underline{\alpha}}), |G|_{e_1 e_2 e_3 \bar{f}_1 \bar{f}_2 \bar{f}_2}) = w^{-4} N^{e_1}_{e_2 e_3} N^{\bar{f}_1}_{\bar{f}_2 \bar{f}_3}. \tag{A.4}$$

This concludes the proof of eq. (2.23).

B Proof of some equations of Section 3

In this appendix we outline the proofs of some equations of Section 3. The following equations involving graphs are to be understood as equations of their invariants in the sense of eq. (2.4). If there are graphs with open lines they have to be interpreted as parts

of closed graphs. By eqs. (2.6)-(2.9) and the Wigner-Eckart relation (2.10) we have the following completeness and Racah relation

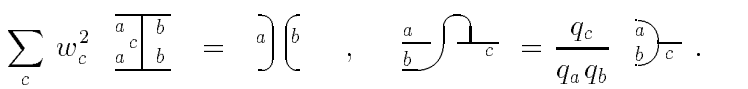

(B.1)

The Verlinde matrix (genus $g = 1$)

$$S_{ab} = (-1)^{2a+2b}\ \frac{\sin\frac{\pi}{r}(2a+1)(2b+1)}{w\ \sin\frac{\pi}{r}} \tag{B.2}$$

diagonalizes the fusion matrix, i.e. it solves the eigenvalue equation

$$(N^d\ S)_{ab} = \frac{S_{db}}{S_{d0}}\ S_{ab} \tag{B.3}$$

and we have the well known relations (see e.g. [15])

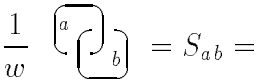

(B.4)

In particular $S^2 = 1$ with the Wigner-Eckart relation (2.10) implies the following change of a part of a graph (compare (A.2) in [15])

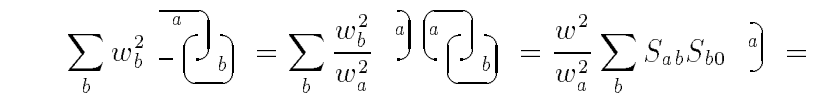

(B.5)

and therefore using the completeness relation (B.1)

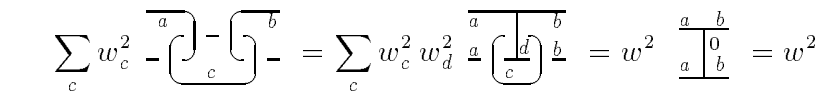

(B.6)

Also we have with eq. (B.1)

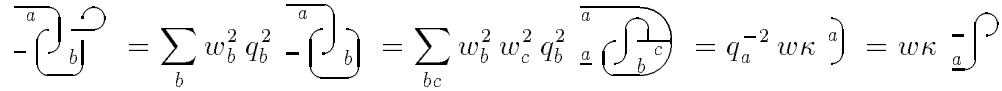

(B.7)

and analogously to eq. (B.6)

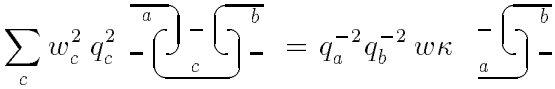

(B.8)

where in both cases the sum over c yields the constant

$$w\kappa = \sum_c w_c^4\ q_c^2 = w\ q^{-3/2}\ e^{-i\pi(1/4+r/2)}. \tag{B.9}$$

In eqs. (B.7) and (B.8) Yang-Baxter relations have been used and for eq. (B.9) Gauss' reciprocity relation. These formulas for the special matrix $S_{ab} = S^0_{ab}$ are now used to derive eqs. (3.55)-(3.58) for the general matrix S^c_{ab} defined by eq. (3.46).

Proof of eqs. (3.54): The symmetry $S^c_{ab} = S^c_{ba}$ follows directly from the homotopy invariance of the invariants of graphs on S^2 and the second equation by

$$\frac{w}{w_a w_b} S^c_{ab} = \quad = \quad = \quad = q_c \frac{w}{w_a w_b} (S^c_{ab})^* \ . \tag{B.10}$$

Proof of eqs. (3.54): Equation (B.6) implies

$$\sum_d S^c_{ad}\, S^{c*}_{db} = \sum_d \frac{w_a\, w_d^2\, w_b}{w^2} \quad = \sum_d \frac{w_a\, w_d^2\, w_b}{w^2} \quad = \delta_{ab}\, N^c_{aa}. \tag{B.11}$$

Proof of eqs. (3.56): Equation (B.8) implies

$$\sum_d S^c_{ad}\, q_d^2\, S^{c*}_{db} = \sum_d \frac{w_a\, w_d^2\, w_b}{w^2} q_d^2 \quad = \sum_d \frac{w_a\, w_d^2\, w_b}{w^2} q_d^2 \quad = \kappa q_a^{-2} q_b^{-2}\, S^{c*}_{ab} \tag{B.12}$$

and eq. (3.56) follows with $S^c_{ab} = S^c_{ba}$.

Proof of eqs. (3.57) and (3.58): The eigenvalue equation of N^{cd}_{ab} defined by eq. (3.53) reads

$$\sum_{a'} N^{cd}_{a'a}\, S^c_{a'b} = \sum_{a'} \frac{w_a\, w_{a'}^2\, w_b}{w^2} \quad = \frac{w_a\, w_b}{w^2} \quad = \frac{S_{db}}{S_{0b}}\, S^c_{ab}. \tag{B.13}$$

Proof of eq. (3.53): Using again eq. (B.1) we obtain the following representation for the matrix S^s_{ab}

$$S^c_{ab} = \frac{w_a\, w_b}{w} \quad = \sum_d w_d^2\, \frac{w_a\, w_b}{w} \quad = \frac{1}{w\, q_a^2\, q_b^2} \sum_d w_d^2\, q_d^2\, N^{cd}_{ab}. \tag{B.14}$$

C Chern-Simons invariants for flat connections

The results of [2] describe explicitly how to obtain all irreducible flat connections up to gauge equivalence of $M_8(-n/m)$ and give precise formulae for computing the corresponding Chern-Simons invariants. Since we derive some consequences from these formulae and

also for the convenience of the reader we will briefly recall these results. The group G of the figure-eight knot has the presentation

$$\langle x, y : [x^{-1}, y]x = y[x^{-1}, y]\rangle$$

with x representing a meridian and $\lambda = [y, x^{-1}][x, y^{-1}]$ the preferred longitudinal curve. Consider the curves $(e^{2\pi is}, u_{\pm}(s)), s \in [1/6, 1/3]$, in $\mathbf{C} \times \mathbf{R}$ given by $u_{\pm}(s) = \cos 4\pi s - 3/2 \pm \sqrt{\cos^2 4\pi s - \cos 4\pi s - 3/4}$. Then the representations of G given by

$$\begin{aligned} x &\longmapsto \begin{pmatrix} e^{2\pi is} & e^{-2\pi is} \\ 0 & e^{-2\pi is} \end{pmatrix} \\ y &\longmapsto \begin{pmatrix} e^{2\pi is} & 0 \\ -e^{2\pi is}u_{\pm}(s) & e^{-2\pi is} \end{pmatrix} \quad , s \in [1/6, 1/3] \end{aligned}$$

are conjugate in $SL(2, \mathbf{C})$ to irreducible $SU(2)$ representations and correspond bijectively to the conjugacy classes of irreducible $SU(2)$ representations.

Actually, the above $SL(2, \mathbf{C})$ representation is conjugate to a unique $SU(2)$ representation which sends

$$x \to \begin{pmatrix} e^{2\pi is} & 0 \\ 0 & e^{-2\pi is} \end{pmatrix} \quad \text{and} \quad \lambda \to \begin{pmatrix} L_{\pm}(s) & 0 \\ 0 & L_{\pm}(s)^{-1} \end{pmatrix}$$

with $L_{\pm}(s) = -1 + e^{-4\pi is} - 2e^{4\pi is} + e^{8\pi is} + u_{\pm}(s) \cdot (e^{-4\pi is} - e^{4\pi is})$. Call this representation $\rho_{s,\pm}$. Let $\rho_{s,\pm}$ be a representation which projects to a representation of $\pi_1(M_8(n/m))$. If $\gamma_t, 0 \leq t \leq 1$, is a path of $SL(2, \mathbf{C})$ representations of G from the identity to $\rho_{s,\pm}$ such that $\gamma_t(x) = \begin{pmatrix} e^{2\pi i\alpha(t)} & 0 \\ 0 & e^{-2\pi i\alpha(t)} \end{pmatrix}$ and $\gamma_t(\lambda) = \begin{pmatrix} e^{2\pi i\beta(t)} & 0 \\ 0 & e^{-2\pi i\beta(t)} \end{pmatrix}$ then the main result of [2], Theorem 4.3, implies that the Chern-Simons invariant $S_{CS}(\rho_{s,\pm})$ of $M_8(n/m)$ corresponding to $\rho_{s,\pm}$ is equal to

$$-2\int_0^1 \beta\alpha' dt - \mu \cdot n\alpha^2(1) - \nu \cdot m\beta^2(1) - 2\mu \cdot m\alpha(1)\beta(1). \tag{C.1}$$

Here μ and ν are integers such that $\nu n - \mu m = 1$. (This is formula (*) of [2], p. 361, taking account of a misprint). On pages 361, 362 of [2] a path of representations from id to $\rho_{1/6,+} = \rho_{1/6,-}$ is provided and the corresponding value of the integral $\int \beta\alpha'$ up to this point is evaluated as $1/12$. The corresponding values of α and β are $1/6$ and $1/2$. The representation $\rho_{s,\pm}, s \in [\frac{1}{6}, \frac{1}{3}]$ of G factors through a representation of $\pi_1(M_8(n/m))$ if and only if $\rho_{s,\pm}(x^n \cdot \lambda^m) = id$, i.e. if and only if

$$e^{-2\pi ins} = (L_{\pm}(s))^m \tag{C.2}$$

Define $\lambda_{\pm}(s)$ by $L_{\pm}(s) = e^{2\pi i\lambda_{\pm}(s)}$ such that $\lambda_{\pm}$ are continuous and $\lambda_{\pm}(1/4) = 0$. One easily sees that $L_{\pm}(\frac{1}{4} - s) = \overline{L_{\pm}(\frac{1}{4} + s)}$ so that $\lambda_{\pm}(\frac{1}{4} - s) = -\lambda_{\pm}(\frac{1}{4} + s)$. Furthermore,

$L_\pm(\frac{1}{4}+s) = -2\sin^2 4\pi s + \cos 4\pi s \pm 2i \sin 4\pi s\sqrt{(\cos 4\pi s + \frac{1}{2})^2 - 1}$. This implies that for $0 \le s \le 1/12$ the function $\lambda_+(1/4+s)$ is strictly monotonously increasing from 0 to $1/2$ and $\lambda_-(s) = -\lambda_+(s)$.

It follows that $\rho_{s,\pm}$ factors through a representation of $M_8(n,m)$ if and only if

$$n/m \cdot s \equiv \pm\lambda_-(s) \mod (1/m). \tag{C.3}$$

The following facts are easy to see (we will always assume that n, m are coprime).

- If n is even, then $1/4+\tau$ is a solution if and only if $1/4-\tau$ is a solution,
- $1/4$ is a solution if and only if 4 divides n,
- if s is a solution for (n,m) then it is also a solution for $(-n,m)$ with the sign in $\rho_{s,\pm}$ changed.

Let $R(n/m,\pm)$ be the number of $s \in [1/6,1/3]$ such that $\rho_{s,\pm}$ projects to a representation of $\pi_1 M_8(n/m)$. We will always assume that $m > 0$. Then

- for $n/m \ge -2\cdot\sqrt{5}$ $(= max\{\lambda'_-(s) : 1/6 \le s \le 1/3\})$ $R(n/m,+)$ is the number of integers in $[-\frac{m}{2}-\frac{n}{3}, \frac{m}{2}-\frac{n}{6}]$.
- for $n/m \le -12$ $R(n/m,+)$ is the number of integers in $[\frac{m}{2}-\frac{n}{6}, -\frac{m}{2}-\frac{n}{3}]$,
- for $n/m \le 2\cdot\sqrt{5}$ $R(n/m,-)$ is the number of integers in $[-\frac{m}{2}-\frac{n}{6}, \frac{m}{2}-\frac{n}{3}]$,
- for $n/m \ge 12$ $R(n/m,-)$ is the number of integers in $[\frac{m}{2}-\frac{n}{3}, -\frac{m}{2}-\frac{n}{6}]$.

To compute the Chern-Simons invariant $S_{CS}(\rho_{s,\pm})$ of $M_8(n/m)$ corresponding to the representation $\rho_{s,\pm}$ we employ (C.1). Using the path of [2] from the trivial representation to $\rho_{1/6,+} = \rho_{1/6,-}$ and then the path $t \mapsto \rho_{t,\pm}, t \in [1/6,s]$, the Chern-Simons invariant of $\rho_{s,+}$ is equal to

$$-2\left(1/12 + \int_{1/6}^{s}(\lambda_+(t)+1)dt\right) - \mu n s^2 - \nu m(\lambda_+(s)+1) - 2\mu m s(\lambda_+(s)+1) \tag{C.4}$$

while the one corresponding to $\rho_{s,-}$ is

$$-2\left(1/12 + \int_{1/6}^{s}\lambda_-(t)dt\right) - \mu n s^2 - \nu m\lambda_-(s) - 2\mu m s\lambda_-(s). \tag{C.5}$$

(Since the curve β of the path from id to $\rho_{1/6,+}$ ends with the value $1/2$, the continuation of β from $\rho_{1/6,+}$ to $\rho_{s,+}$ is $\lambda_+(s)+1$, and not simply $\lambda_+(s)$).

Using these formulae and the fact that $\lambda_\pm(1/4+\tau) = -\lambda_\pm(1/4-\tau)$ it is a straight forward calculation that for even n and $s = 1/4+\tau$ a solution of eq. (C.3) we obtain $S_{CS}(\rho_{1/4+\tau,\pm}) - S_{CS}(\rho_{1/4-\tau,\pm}) \equiv n\mu/4 \ mod\ 1$, where as before μ is given by $\nu n - \mu m = 1$. Therefore, we obtain

Proposition C.1 *(a) Let n, m be coprime with $n = 4k+2$. Then for any irreducible representation $\rho_{1/4+\tau,\pm}$ of $\pi_1(M_8(n/m))$ also $\rho_{1/4-\tau,\pm}$ is an irreducible representation and*

$$S_{CS}(\rho_{1/4+\tau,\pm}) - S_{CS}(\rho_{1/4-\tau,\pm}) = 1/2 \ mod\ 1.$$

(b) if $n = 4k$, then we have the irreducible representations $\rho_{1/4,\pm}$ with Chern-Simons invariant

$$\pm 1/5 + \ell/4 \quad if \ \ k \equiv \ell \ mod\ 4$$

and for any irreducible representation $\rho_{1/4+\tau,\pm}$ of $\pi_1(M_8(n/m))$ also $\rho_{1/4-\tau,\pm}$ is an irreducible representation and

$$S_{CS}(\rho_{1/4+\tau,\pm}) = S_{CS}(\rho_{1/4-\tau,\pm}).$$

Proposition C.1 was inspired by our numerical results. First, our numerical calculations of $Z_l(M_8(-n/1), r)$ for $n \equiv 2 \ mod\, 4$ suggested that these numbers are 0 for all odd r. Then we proved this analytically (see Appendix D). This implies that the Fourier transform $\tilde{Z}_l(M_8(-n/1), t)$ is periodic with period $1/2$. Assuming the correctness of the semiclassical approximation formula (5.90) a statement like Proposition C.1 would have to hold.

The statement that $Z_l(M_8(-n,1), r) = 0$ for $n \equiv 2 \ mod\, 4$ and r odd may be generalized as follows

Proposition C.2 *Let $M_{\mathcal{K}}(n/m)$ be the 3-manifold obtained by (n/m)-Dehn surgery on the knot $\mathcal{K} \subset S^3$. If $n \equiv 2 \ mod\, 4$ (and m, n coprime) then $Z_l(M_{\mathcal{K}}(n/m), r) = 0$ for every odd r.*

Remark C.3 *In case $\mathcal{K}$ is the figure eight-knot, this result turns into an if and only if with a proof which uses different arguments (see Appendix D).*

Proof. By [7], Corollary 8.9, if suffices to show that $Z_l(M_K(4k+2/2\ell+1), 3) = 0$ which in turn holds if and only if one can embed a closed surface of odd Euler characteristic into $M_K(4k+2/2\ell+1)$ ([7], Theorem 6.3). If $D^2 \times S^1$ is the solid torus glued into the exterior of a tubular neighborhood of K to obtain $M_K(4k+2/2\ell+1)$ then a Seifert surface of K will meet the boundary torus $S^1 \times S^1$ of $D^2 \times S^1$ in a simple closed curve homologous to $-p(S^1 \times \{*\}) + (4k+2)(\{*\} \times S^1)$, where p is an integer such that $p(2\ell+1) \equiv$

$-1\ mod\,(4k{+}2)$. Any such curve bounds a non-orientable surface of genus $2k{+}1$ in $D^2\times S^1$. The union of these two surfaces is then a closed surface of odd Euler characteristic.

With regard to reducible representations note that the first integral homology group of $M_8(n/m)$ is isomorphic to $\mathbf{Z}/n\mathbf{Z}$. Therefore, $\pi_1(M_8(n/m))$ has non-trivial reducible SU(2) representations if $|n|>1$. These correspond to the representations of $\pi_1(L(n,m))$ where $L(n,m)$ is the (n,m)-lens space. The proof of Theorem 5.1 of [2] can be applied to calculate the set of Chern-Simons invariants of reducible representations of $M_K(n/m)$ for any knot K in S^3. Therefore, the set of Chern-Simons invariants of $M_K(n/m)$ corresponding to reducible flat connections A (for these, as noted in Section 5, $\dim H^0(A)=1$ unless A is trivial) is given by

$$\left\{-\frac{t^2p}{n}\;\Big|\;t=0,1,\ldots,\left[\frac{n}{2}\right]\right\}, \tag{C.6}$$

where as before p is an integer such that $p\cdot m\equiv -1\ mod\ n$.

D Vanishing invariants

In this appendix we give a necessary and sufficient condition for $Z_l(M_8(-n/m),r=3)$ to vanish. Notice that by a result of Kirby and Melvin [7] $Z_\ell(M_8(-n/m),r)$ vanishes for r odd whenever $Z_l(M_8(-n/m),r=3)=0$.

For $r=3$ we have

$$A=\begin{pmatrix}1 & & 0\\ 0 & - & i\end{pmatrix}\ ,\quad S=\frac{1}{\sqrt{2}}\begin{pmatrix}1 & -1\\ -1 & -1\end{pmatrix}$$

and

$$\begin{vmatrix}e & e & 0\\ e & e & 0\end{vmatrix}=(-1)^{2e}=wS_{0e}\quad,\quad e=0,\frac{1}{2}.$$

We consider the case $|\frac{n}{m}|>1$ first.

Since $S^2=\mathbf{1}$ we have by (74) and (80)

$$\begin{aligned}Z_l(M_8(-n/m),r=3) &= e^{i\psi}w^{-1}\sum_e(-1)^{2e}\langle e|A^{m_t}S\cdots SA^{m_1}S|0\rangle\\ &= e^{i\psi}\langle 0|SA^{m_t}S\cdots SA^{m_1}S|0\rangle\end{aligned}$$

where $(m_t,\cdots m_1)$ is the continued fraction expansion of n/m (cf. sect. 4). Consider $X(m_t,\cdots m_1)=SA^{m_t}S\cdots SA^{m_1}S$ as a word in S and A. We call words of the form

$$\begin{aligned}&SA^\alpha SA^k\quad(\alpha\text{ even})\\ &SA^\alpha SA^{\beta_r}\cdots SA^{\beta_1}SA^\gamma SA^k(\alpha,\gamma\ \text{ odd},\beta_j\text{ even},0\le r)\end{aligned}$$

initial factors if $k \neq 0$ and final factors if $k = 0$. A (final or initial) factor of the form $SA^{4k}SA^k$ or of the form $SA^\alpha SA^{\beta r} \cdots SA^{\beta_1} SA^\gamma SA^k$ with $\gamma \equiv \alpha \ mod \ 4$ is called even, all other factors are called odd. $X(m_t, \cdots m_1)$ can be written uniquely in the form

$$I_p \cdots I_1 \cdot F \ \text{ or}$$
$$I_p \cdots I_1 \cdot SA^\gamma S \ \ (\gamma \text{ odd}) \text{ or}$$
$$SA^\alpha SA^{\beta_r} \cdots SA^{\beta_1} S \ (\alpha \text{ odd}, \beta_j \text{ even})$$

where the I_j are initial factors and F is a final factor.

Lemma D.1 *Let $|n/m| > 1$. $Z_l(M_8(-n/m), r = 3) = e^{i\psi}\langle 0|X(m_t, \cdots m_1)|0\rangle$ vanishes if and only if $X(m_t, \cdots m_1) = I_p \cdots I_1 \cdot F$ where the I_j are initial factors, F is a final factor and the number of odd factors is odd.*

Proof: Use the fact that $A^4 = 1$ and $(SA^2)^4 = -\mathbf{1}$ to check that even factors are diagonal matrices with both diagonal entries different from zero while odd factors are off-diagonal matrices with both off diagonal entries different from zero (since their determinant is $\neq 0$). The lemma follows from the equations

$$SAS = \frac{1}{2}\begin{pmatrix} 1-i & -1-i \\ -1-i & 1-i \end{pmatrix}; SA^3S = \frac{1}{2}\begin{pmatrix} 1+i & -1+i \\ -1+i & 1+i \end{pmatrix}$$

and

$SA^\alpha SA^{\beta_r} \cdots SA^{\beta_1} S = SA^\alpha SA^{\beta_r} \cdots SA^{\beta_1} SA^\alpha SSA^{4-\alpha} = D \ SA^{4-\alpha}$ with D diagonal. For all odd α all entries of $SA^{4-\alpha}$ are nonzero.

When comparing Lemma D.1 with Proposition C.2 it turns out that in the case of Dehn surgery on the figure 8 knot Proposition C.2 gives exactly the surgery coefficients for which $Z_l(M_8(-n/m), r = 3)$ vanishes. In fact we have with the notation above

Lemma D.2 *Let $(m_t, \cdots m_1)$ be the continued fraction expansion of n/m ($|n/m| > 1$) and let $X(m_t, \cdots m_1)$ be*

(i) $I_p \cdots I_1 \cdot F$ or

(ii) $I_p \cdots I_1 SA^\alpha S$ (α odd) or

(iii) $SA^\alpha SA^{\beta_r} \cdots SA^{\beta_1} S$($\alpha$ odd, β_j even)

Then $n/m = \frac{4k}{2l+1}$ if and only if case (i) occurs with an even number of odd factors, $n/m = \frac{4k+2}{2l+1}$ if and only if case (i) occurs with an odd number of odd factors.

Proof: We use induction on the length t of the continued fraction expansion. With

$$\begin{aligned} \frac{n}{m} &= m_t - \cfrac{1}{m_{t-1} - \cfrac{1}{\cdots - \cfrac{1}{m_1}}} \\ &= m_t - \cfrac{1}{m_{t-1} - \cfrac{1}{\cdots - \cfrac{1}{m_{s+1} - \frac{1}{q}}}} \end{aligned}$$

where $(m_s, \ldots, m_1)$ is the continued fraction expansion of q. Notice that denominator and numerator of a number described by a continued fraction expansion both change additively by multiples of 4 if the coefficients are changed additively by multiples of 4. Then check that if $SA^{\alpha}SA^{k}$ or $SA^{\alpha} \quad SA^{\beta_r}...SA^{\beta_1}SA^{\gamma}S$ is an even or odd factor and $q = \frac{2a}{2l+1}$, then

$$\alpha - \frac{1}{i - \frac{1}{q}} \quad \text{or} \quad \alpha - \frac{1}{\beta_r - \frac{1}{\cdots - \frac{1}{\gamma - \frac{1}{q}}}}$$

is of the form $\frac{2a'}{2l'+1}$ with $2a' \equiv 2a \; mod \; 4$ and $2a' \equiv 2a+2 \; mod \; 4$ respectively. Analogously a final factor represents a fraction of the form $\frac{2b}{2l+1}$ with b even or odd according to whether the final factor is even or odd. In case (ii) the induction starts with $q = \alpha = odd$. The induction step of adding as above the coefficients of an initial factor to the coefficients of q will change a fraction q of the form odd/something into a q' of the same form.

Finally a direct calculation shows that the fraction represented by $(\alpha, 2, 2, 2, \ldots)$ equals $(\alpha(k+1) - k)/(k+1)$, where k is the number of 2's. If α is odd, then so is $\alpha(k+1) - k$. This takes care of case (iii), concluding the proof of the lemma.

Completely analogous results hold for the case $|\frac{n}{m}| < 1$. Then

$$Z_l(M_8(-n/m), r = 3) = e^{i\psi}\langle 0|A^{m_t}SA^{m_{t-1}} \cdots SA^{m_1}S|0\rangle$$

where now $(m_t, ...m_1)$ is the continued fraction expansion for $|\frac{m}{n}|$. Due to the above form of A when $r = 3$, we have

$$\langle 0|A^{m_t}SA^{m_{t-1}} \cdots SA^{m_1}S|0\rangle = \langle 0|SA^{m_{t-1}} \cdots SA^{m_1}S|0\rangle.$$

Therefore $(m_{t-1}, \cdots m_1)$ is the continued fraction expansion of $|n|/(m_t|n| - |m|)$ with $|n| > m_t|n| - |m| > 0$. Thus $\frac{n}{m}$ is of the form $4k$/odd, $(4k+2)$/odd or odd/something if and only if $|n|/(m_t|n| - |m|)$ is.

References

[1] Witten, E.: Quantum field theory and the Jones polynomials, Commun.Math.Phys. **121**, 351-399 (1989).

[2] Kirk,P.A., Klassen, E.P., Chern-Simons invariants of 3-manifolds and representations of knot groups, Math. Ann. **287**, 343-367 (1990).

[3] Fröhlich, J., King, C.: The Chern-Simons theory and knot polynomials, Commun. Math. Phys. **126**, 167-199 (1989).

[4] Jones, V.F.R., A polynomial invariant for links via von Neumann algebras, Bull. AMS **12** 103-111 (1985);

Hecke algebra representations of braid groups and link polynomials, Ann. Math. **126** 335-388 (1987).

[5] Reshetikhin, N.Yu., Turaev, V.G.: Ribbon graphs and their invariants derived from quantum groups, Commun.Math.Phys. **127**, 1-26 (1990).

[6] Reshetikhin, N.Yu., Turaev, V.G.: Invariants of 3-manifolds via link polynomials and quantum groups, Inv.Math. **103**, 547-597 (1991).

[7] Kirby, R., Melvin, P.: The 3-manifold invariants of Witten and Reshetikhin-Turaev for $sl(2, \mathbf{C})$, Inv. Math. **105**, 473-545 (1991).

[8] Turaev, V.G., Viro, O.Y.: State sum of 3-manifolds and quantum 6j-symbols, Topology **31**, 865-902 (1992).

[9] Turaev, V.G.: Topology of shadows (preprint 1991)

[10] Turaev,V.G.: Quantum invariants of 3-manifolds I and II, Strassbourg-preprint 509/p-295 and 1992/015

Turaev, V.G.: Quantum invariants of 3-manifolds and a glimpse of shadow topology, C.R.Acad.Sci. Paris 313, Ser. I, 395-398 (1991).

Turaev, V.G.: Quantum invariants of links and 3-valent graphs in 3-manifolds, Publ. Math. (IHES) **77**, 121-171 (1993).

Turaev, V.G.: State sums in low-dimensional topology, Proc. ICM, Kyoto, 1990 Vol. **1**, 689-698 (1991).

[11] Durhuus, B.,Jacobsen, H., Nest, R.: Topological quantum field theories from generalized 6j-symbols, Rev. Math. Phys. **5**, 1-67 (1993).

[12] Durhuus, B.:A discrete approach to topological quantum field theories, J. Geom. and Phys. II, 155-180 (1993).

[13] Walker, K.: On Witten's three-manifold invariants, preprint (1991).

[14] Karowski, M., Müller, W., Schrader, R.: State sum invariants of compact 3 manifolds with boundary and 6j-symbols, J. Phys. A: Math. Gen. **25**, 4847-4860 (1992).

[15] Karowski, M., Schrader, R.: A combinatorial approach to topological quantum field theories and invariants of graphs, Commun. Math. Phys. **151**, 335-402 (1993).

[16] Osterwalder, K., Schrader, R., Axioms for euclidian Green's functions I,II Commun. Math. Phys. **31**, 83-112 (1973), **42**, 281-305 (1975).

[17] Beliakova, A., Durhuus, B.,Topological quantum field theory and invariants of graphs for quantum groups, Commun. Math. Phys. **167**, 395-429 (1995).

[18] Gepner, D., Witten, E.: String theory on group manifolds, Nucl. Phys. **B278**, 493-549 (1986).

[19] Freed, D., Gompf, R.E.: Computer calculation of Witten's 3-manifold invariant, Commun.Math.Phys. **141**, 79-117 (1991).

[20] Jeffrey, L.C.: Chern-Simons-Witten invariants of Lens spaces and torus bundles, and the semiclassical approximation, Commun.Math.Phys. **147**, 563-604 (1992).

[21] Atiyah, M., On framings of 3-manifolds, Topology **29**, 1-8 (1990).

[22] Moore, G., Seiberg, N.: Classical and quantum conformal field theory, Commun.Math.Phys. **123**, 177-254 (1989).

[23] Kohno, T.: Topological invariants for 3-manifolds using representations of mapping class groups I, Topology **31**, 203-230 (1992) and Contemp. Math (AMS) (to appear).

[24] Spanier, E.H., Algebraic Topology, New York, Mac Graw Hill (1966)

[25] Karowski, M.:Topological quantum field theories in terms of coloured graphs associated to quantum groups, in 'Anales de Fisica, Monografias 1, Group Theoretical Methods in Physics, Vol II', p. 118, ed. M.A.del Olmo et al, Ciemat, Madrid 1992.

[26] Wajnrub, B.: A simple presentation for the mapping class group of an orientable surface, Israel Journ. of Mathematics, **45**, 157-174 (1983).

[27] Hegaard, P., Sur l'Analysis situs Bull. Soc. Math. France **44** 161-242 (1916).

[28] Wenzl, H., Braids and invariants of 3-manifolds, Inv. Math. **114**, 235-275 (1993).

[29] Kirillov, A.N., Reshetikhin, N.Yu.: Representation of the Algebra $U_q(s\ell(2))$, q-orthogonal Polynomials and invariants of links, in "New Developments in the Theory of Knots", T. Kohno (ed.), Advances series in Mathematical Physics Vol. 11, World Scientific, Singapore: 1989.